공학박사 학위논문

테트라포드 나노입자의 분산 구조 제어 및 평가

Control and Evaluation of Dispersion Structure of Tetrapod Nanoparticles

2016 년 8 월

서울대학교 대학원

화학 생물 공학부

서 석 규

Control and Evaluation of Dispersion Structure of Tetrapod Nanoparticles

테트라포드 나노입자의 분산 구조 제어 및 평가

지도 교수 차 국 헌

이 논문을 공학박사 학위논문으로 제출함

2015 년 12 월

서울대학교 대학원

화학 생물 공학부

서 석 규

서석규의 공학박사 학위논문을 인준함

2015 년 12 월

위 원 장 _____ (인)

부위원장 _____ (인)

위 원 _____ (인)

위 원 _____ (인)

위 원 _____ (인)

Abstract

Inorganic nanoparticles have the unique electric and optical properties which is determined by their size and shapes, thus various researches about the synthesis of well-defined nanoparticles as well as the analysis of their functionality for the diverse applications. Especially tetrapod nanocrystals are greatly interested because of their large surface area for junction with neighboring materials and formability of interconnected structures from their unique structural feature.

Meanwhile, dispersion of inorganic nanoparticles within polymer matrix is most important for full development of their unique properties. Surface modification of inorganic nanoparticles with organic polymers is one way to make well-dispersed inorganic nanoparticle/polymer system. However, even though various techniques for control the dispersion structure have been studied, these are hardly certified as the reliable method without accurate evaluation of dispersion structure. Typically, microscopic method has been used for characterization of dispersion structure. However, recently, scattering methods is not only used for the complement but also the alternative to characterize the structural properties, due to the detectability about ensemble averages of dispersion structure.

Therefore we characterize the dispersion structure of tetrapod using scattering method, and control the dispersion structure of tetrapod nanoparticles by hybridization.

The features of tetrapod nanocrystals, organic/inorganic hybridization and characterization of dispersion structure using scattering method are introduced in chapter 1.

In chapter 2, scattering model for tetrapod is presented by theoretical calculation for characterization of dispersion structure of tetrapod nanocrystals. Geometry of tetrapod is simplified using regularity of identical four cylindrical arms with tetrahedral include angles. Because anisotropic tetrapod needs three rotations for considering the random orientations, additional rotation about bisector of tetrapod is considered. Scattering intensity and their pair distance distribution functions of presented model are calculated numerically. Verification about scattering model is proved by numerical calculation and simulation as well as small angle x-ray scattering experiment of tetrapod dispersed in solvent.

In chapter 3, dispersion structure of tetrapod nanoparticles dispersed within polymer matrix is characterized using small angle x-ray scattering. Because dispersion of inorganic nanocrystals within polymer matrices is regarded as the most important for full realization of unique properties of inorganic materials, the dispersion structure has to be characterized preferentially. Scattering intensity from colloidal structure is consist with form factor, which informs the size and shape of particles and structure factor, which contains the correlational information between particles. Form factor of tetrapod is obtained from dilute solution of tetrapod dispersed within good solvent to exclude the correlational effects. Dispersion structure of correlation between particles, structure factor, is deduced by dividing the total scattering intensity by form factor. In order to compare the differences between well-dispersed structure and aggregated structure, SAXS is performed for hybrid, which is the composite of surface modified tetrapod and matrix polymer, and simple blends

without surface modification. Comparing the structure factors of hybrid and blends, it is found that dispersion structure is not only analyzable but also quantitatively comparable by scattering method.

In chapter 4, method for control of the dispersion structure of tetrapod nanoparticles within polymer matrix as well as polymer particles is presented. polystyrene-b-poly(cysteamine methyl disulfide) diblock copolymer, which are synthesized for surface modification of tetrapod nanocrystals by RAFT polymerization, facilitate the amphipathic properties due to polystyrene main chain and amide functional groups. Therefore, they forms the globular polymer particles in polar solvent, while polystyrene homopolymers are precipitated quickly. When the block copolymer is particulated in company with tetrapod nanoparticles, tetrapods are incorporated to polymer particles. It is found that size of the polymer particles are controlled by concentration of block copolymers and solvent polarity and the number of tetrapod per polymer particle is also controlled by weight ratio of polymer and tetrapod nanoparticle.

These series of studies about the control and evaluation of the dispersion structures are present the approaching way to apply the tetrapod nanocrystals for various fields, which need the controllability of dispersion structures, like the solar cells as well as the transistors.

Keyword : Tetrapod nanoparticle, Block copolymer, Hybrid, Small Angle X-ray Scattering, Dispersion Structure
Student Number : 2012-30255

Table of Contents

List of Figures

Chapter 1. Introduction

1.1. Tetrapod Nanoparticles

Inorganic nanoparticles have been studied for various applications due to their unique electrical[1,2] and optical[3] properties which are different with in bulk state. Since the properties of nanoparticles are originated from the quantum confinement effect, these properties can be easily modified by controlling its size and shape. Therefore, the efforts for revealing the geometry-properties relationship of nanoparticles and synthesizing the well-defined nanoparticles with relatively large amount have been proceeded[1-9].

Especially, the tetrapod nanoparticles have shown better light absorption, exciton dissociation and charge transfer properties than the QDs and nanorods because of their unique geometry which is four identical cylindrical arms stretched out with tetrahedral angle. Due to their distinctive structure, the tetrapod nanoparticles secure the large surface area for interaction with surround and connection between tetrapod nanoparticles for transportation of charge carriers. [10]

Furthermore, since the scalable synthesis of tetrapod nanoparticles with high uniformity was allowed by the continuous precursor injection method[10], the research about tetrapod nanocrystal has gathered steam for fundamental understanding of the properties induced by distinctive structure as well as for various applications.

1.2. Organic/Inorganic Hybridization and Its Dispersion

Hybridization of organic polymer and inorganic nanoparticles realizes the fusion materials which have the properties of high functional inorganic nanomaterials and organic polymers allowing the high processability with synergetic effects. Therefore the organic/inorganic hybrid materials have huge potentials for diverse applications like as optoelectronic devices[11-17], light emitting diode and biological assay[18,19].

Surface modification of inorganic nanomaterials with organic polymers is feasible method for materialization of organic/inorganic hybridization[20-23]. Hybrid nanomaterials which made by this method also have the advantage of dispersion within organic matrices because the polymers being cover the nanomaterials would enhance or control the compatibility with organic matrices. Therefore, the hybridized nanoparticles covered with polymers (brush polymer) via surface modification facilitate the controllability of distribution structure of nanoparticles within polymer matrices (matrix polymer).

There are two typical options for surface modification of inorganic nanomaterials; "Grafting-from" and "Grafting-to". "Grafting-from" is the surface modification method whose brush polymer is grown from the initiator being at the surface of nanomaterials, typically by controlled radical polymerization[24-30] due to the control of molecular weight of brush polymers. Meanwhile, "Grafting-to" is the method of exchanging the ligands with brush polymer or attaching the brush polymer onto the surface of bare nanomaterials.

Although the areal chain density of brush polymer by "Grafting-to" is relatively lower and easier to control than by "Grafting-from" due to the steric hindrance[31], we mainly used the "Grafting-to" method for hybridization of inorganic nanomaterials because the molecular weight and polydispersity of brush polymer can be controlled[31] easily as well as the process

for hybridization, which is introduction of brush polymer to nanomaterials, is relatively simple than “Grafting-from” method.

Nevertheless, aggregated nanoparticles cannot appeal their own unique properties came from the nanoscale dimension. In order to utilize the unique properties of nanoparticles effectively, the control of dispersion structure is most essential. However, the surface modification of inorganic nanomaterials with organic polymer does not always mean the well-dispersion of inorganic nanomaterials because the dispersion of hybrid nanoparticles governed by thermodynamics, both enthalpic and entropic energy, which are determined by the relationship between brush and matric polymer as well as nanoparticle. Brush polymers onto the surface of inorganic nanomaterials act as a compatibilizer and decrease the enthalpy of the system due to the decrease of the Flory-Huggins interaction parameter[32], which means that the modification of inorganic nanomaterials with organic polymer positively affect the dispersion of hybrid nanomaterials within organic matrices. Entropy is also principle factor for controlling the dispersion structure of hybrid nanoparticles within matrices, however the effect on the dispersion is different with enthalpy and it depends on the chain length of brush polymer, matrix polymer and their ratio as well as grafting chain density. Leibler and co-workers[33] disclosed that free chains of matrix can penetrate into the gap between grafting polymer brushes on nanoparticles when , and then, it results homogeneous dispersion of hybrid nanoparticles within polymer matrix, which is called “wet brush”. On the contrary, depletion of matrix polymer occurs at brush polymer layers when , and consequently, hybrid nanoparticles are aggregated to minimize the contact area and surface energy, which is called “dry brush”.

1.3. Scattering Method for Characterization of Nanoparticles

Typically, dispersion structure of inorganic nanoparticles has been characterized by microscopic methods, which cannot provide the ensemble average fundamentally. However, because the dispersion is a criteria that is not able to be represented by a certain number but by an ensemble average, evaluation of dispersion structure needs the complements of the microscopic methods. Recently, the scattering methods is not used only for the complement of microscopic analysis for characterization of dispersion but also for the alternative method independently, due to its detectability for the ensemble averages of dispersion structure.

Scattering techniques are one of the most powerful tools for characterizing the structural properties of colloidal system[34, 35] because scattered light from particles which have certain geometry contains the structural information of the particle and the feature of correlations between particles.

In order to find the dispersion structure, intensity of scattered light should be separated into two terms; "Form Factor" which have the structural information of single particle and "Structure Factor" which is contain the special distance between particles. For the dispersion structure of nanoparticles, therefore, "Form Factor" of particles must be figured out in advance, and then deduced from total intensity of scattered light. Besides, the "Form Factor" of nanoparticles helpful to determine the dimensions of geometry by fitting with experimental scatting result of dilute condition, which has no correlation effect between particles.

"Form Factor" of particles having certain geometry is resulted from its theoretical scattering model. Because the scatting intensity curves are the Fourier transform of scattering centers, "Form Factor" is the Fourier transform of position

vectors which represent the geometry of single particle. Theoretical models for diverse geometries, from the simple like sphere, cylinder and ellipsoid to the advanced like hollow, core–shell and spheroidal– or globular– end cylinder, (whose geometry has at least one axisymmetry), have been presented by Guinier & Fournet (1955)[36] and also found in the review paper of J. Pedersen (1997)[37] (Figure1.1). However the scattering models for anisotropic structures without axisymmetry, like tetrapod, were scarcely ever presented.

The scattering intensity is the absolute square of scattering amplitude which is calculated by Fourier Transform of position vectors, however the position vectors of anisotropic structure is hard to present in there dimensional space mathematically. Moreover, the consideration of random orientation of particles complicates these mathematical job awfully.

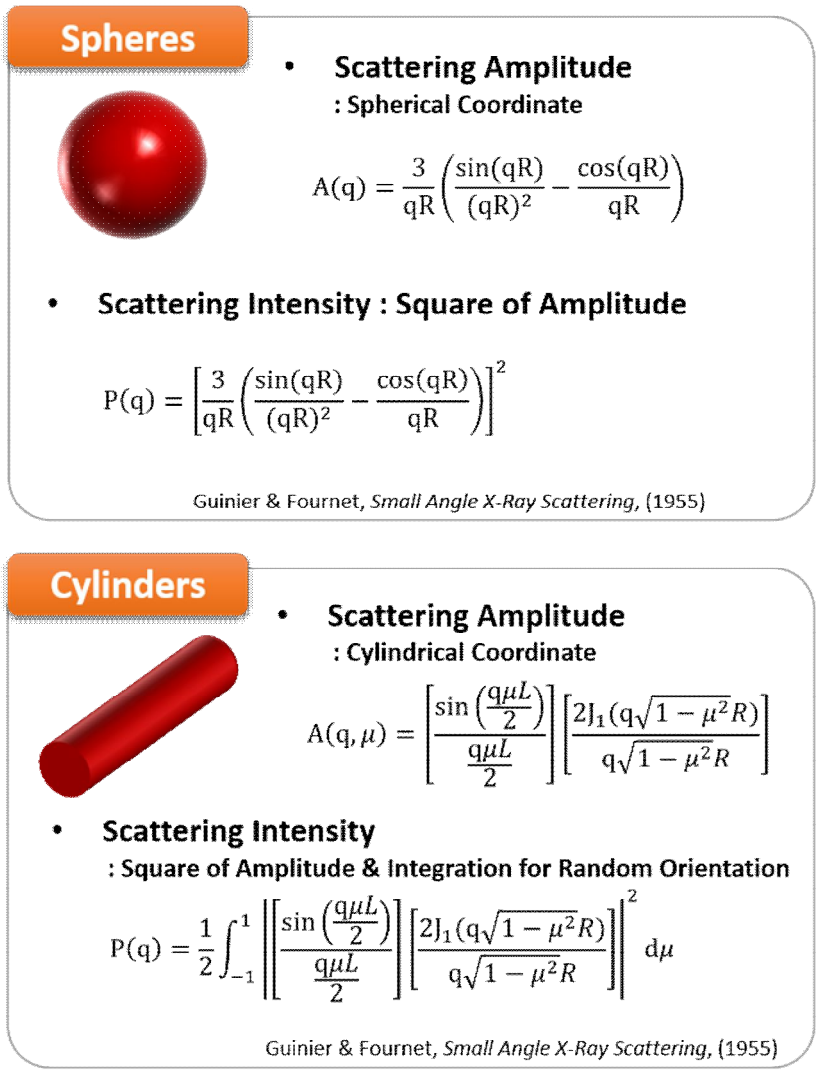

Figure 1.1 Scattering models for sphere and cylinder particles and its scattering functions.

1.4. References

(1) Peng, P.; Milliron, D. J.; Hughes, S. M.; Johnson, J. C.; Alivisatos, A. P.; Saykally, R. J. Nano Lett. 2005, 5 (9), 1809-1813.

(2) Malkmus, S.; Kudera, S.; Manna, L.; Parak, W. J.; Braun, M. J. Phys. Chem. C 2006, 110 (35).

(3) Greenham, N.C.; Peng, X.; Alivisatos, A. P. Phys. Rev. B, 1996, 54, (24), 17628

(4) Lo, S. S.; Mirkovic, T.; Chuang, C.-H.; Burda, C.; Scholes, G. D. Adv. Mater. 2011, 23 (2), 180-197.

(5) Li, J.; Wang. Nano Lett. 2003, 3 (10), 1357-1363.

(6) Choi, C. L.; Li, H.; Olson, A. C. K.; Jain, P. K.; Sivasankar, S.; Alivisatos, A. P. Nano Lett. 2011, 11 (6), 2358-2362.

(7) Amirav, L.; Alivisatos, A. P. J. Phys. Chem. Lett. 2010, 1 (7), 1051-1054.

(8) Miszta, K.; de Graaf, J.; Bertoni, G.; Dorfs, D.; Brescia, R.; Marras, S.; Ceseracciu, L.; Cingolani, R.; van Roij, R.; Dijkstra, M.; Manna, L. Nat. Mater. 2011, 10 (11), 872-876.

(9) Li, F.; Josephson, D. P.; Stein, A. Angew. Chem., Int. Ed. 2011, 50 (2), 360-388.

(10) Jaehoon Lim, Kookheon Char Chem. Mater. 2013, 25, 1443-1449.

(11) Cui, Y.; Banin, U.; Bjo¨rk, M. T.; Alivisatos, A. P. Nano Lett. 2005, 5 (7), 1519-1523.

(12) Sun, B.; Marx, E.; Greenham, N. C. Nano Lett. 2003, 3 (7), 961-963.

(13) Li, Y.; Mastria, R.; Fiore, A.; Nobile, C.; Yin, L.; Biasiucci, M.; Cheng, G.; Cucolo, A. M.; Cingolani, R.; Manna, L.; Gigli, G. Adv. Mater. 2009, 21 (44), 4461-4466.

(14) Dayal, S.; Reese, M. O.; Ferguson, A. J.; Ginley, D. S.; Rumbles, G.; Kopidakis, N. Adv. Funct. Mater. 2010, 20 (16), 2629-2635.

(15) Chen, H.-C.; Lai, C.-W.; Wu, I. C.; Pan, H.-R.; Chen, I. W.

P.; Peng, Y.-K.; Liu, C.-L.; Chen, C.-h.; Chou, P.-T. Adv. Mater. 2011, 23 (45), 5451-5455.
(16) Dayal, S.; Kopidakis, N.; Olson, D. C.; Ginley, D. S.; Rumbles, G. Nano Lett. 2009, 10 (1), 239-242.
(17) Choi, C. L.; Koski, K. J.; Sivasankar, S.; Alivisatos, A. P. Nano Lett. 2009, 9 (10), 3544-3549.
(18) Lim, J.; Bae, W. K.; Lee, D.; Nam, M. K.; Jung, J.; Lee, C.; Char, K.; Lee, S. Chem. Mater. 2011, 23 (20), 4459-4463.
(19) Kwak, J.; Bae, W. K.; Lee, D.; Park, I.; Lim, J.; Park, M.; Cho, H.; Woo, H.; Yoon, D. Y.; Char, K.; Lee, S.; Lee, C. Nano Lett. 2012, 12 (5), 2362-2366.
(20) Matthias Zorn, Kookheon Char, ACS NANO, 2009, VOL. 3, NO. 5, 1063-1068.
(21) Dongkyu Kim, Sangyong Jon, Nanotechnology 22 (2011) 155101 (22) Ohno, K.; Morinaga, T.; Koh, K.; Tsuiji, Y.; Fukuda, T.; Macromolecules 2005, 38 ,(6), 2137-2142.
(22) Paschalis Alexandridis, Chem. Eng. Technol. 2011, 34, No. 1, 15-28.
(23) Rudolf Zentel, Matthias Zorn, Nano Lett. 2010, 10, 2812-2816.
(24) Pyun, J.; Matyjaszewski, K. ; Kowalewdki, T.; Savin, D,; Patterson, G.; Kickelbick, G,; Huesing, N. J. Am.chem. soc. 2001, 123 (38), 9445-9446.
(25) Ohno, K.; Morinaga, T.; Koh, K.; Tsuiji, Y.; Fukuda, T.; Macromolecules 2005, 38 ,(6), 2137-2142.
(26) Blomberg, S.; Harth, E.; Bosman, A. W.; Vam Horn, B.; Hawker, C. J. polm. Sci., Part A : Polym. Chem. 2002, 40, (9), 1309-1320.
(27) Baetholome, C.; Beyou, E.; Bourgeat-Lami, E.; Chaumont, P.; Zydowicz, N. Macromolecules, 2003, 36, (21), 7946-7952.
(28) Randjan, R.; Brittain, W. J. Macromolecules, 2007, 40, (17), 6217-6223.
(29) Ranjan, R,; Brittain, W. J. Macromol. Rapid comm., 2008, 29, (12-13), 1104-1110.
(30) Li, C.; Bemicewicz, B. C. Macromolecules, 2005, 38, (14), 55929-59363.

(31) Qin, S.; Qin, D.; Ford, W. T.; Resasco, D. E.; Herrera, J. E. Macromoleculs, 2004, 37, (3), 752-757.
(32) Borukhov, I.; Leibler, L. Macromolecules, 2002, 35, (13), 5171-5182.
(33) Ferreira, P. G.; Ajdari. A.; Leibler, L. Macromolecules, 1998, 31, (12), 3994-4003.
(34) Carsten Svaneborg and Jan Skov Pedersen, THE JOURNAL OF CHEMICAL PHYSICS, 2012, 136, 104105
(35) Carsten Svaneborg and Jan Skov Pedersen, THE JOURNAL OF CHEMICAL PHYSICS, 2012, 136, 154907.
(36) Guinier & Fournet, Small Angle X-Ray Scattering, (1955)
(37) J.S. Pedersen, Adv. Colloid Interface Sci. 70 (1997) 171.

Chapter 2. Scattering Model for Tetrapod

2.1. Introduction

Tetrapod nanoparticles, due to their distinctive structure which is formed by four identical cylinders (arms) stretched out with same included angles, has been expected to facilitate the versatile features, like the transportation of charge carriers and the efficient interaction with surround[1].

Just like other nanoparticles, characterization of size and shape for tetrapod nanoparticles is also important because they determine the properties of inorganic nanoparticles. In this respect, scattering techniques would be the best option for characterization of nanoparticles because they are powerful tools[2,3] to investigate the structure property of particles dispersed within matrices because the light scattered by particles informs the structural property of the particle and the feature of correlations between particles. Since intensity of scattered light is the Fourier transform function of distance between scattering centers, the scattering intensity would rather be fitted by theoretical model than be itself for the sensible interpretation. Theoretical models for diverse geometries, from the simple like sphere, cylinder and ellipsoid to the advanced like hollow, core−shell and spheroidal− or globular−end cylinder, have been well known[4,5] while the scattering models for anisotropic structures were scarcely ever presented.

Because, in order to deduce the theoretical model, the relevant position vector of objects should be specified in three dimensional coordinate system to consider the volumetric geometry as well as the random orientation mathematically[6], however, in the case of anisotropic structure, specification of the position vector is highly complicated, besides it is rarely possible to consider the random orientation. For the tetrapod, however, though it is anisotropic,

specification of the position vector and consideration of the random orientation is available since it has structural characteristics which are consist with four identical arms with same included angles. In this work, the scattering model for tetrapod is presented and simplified by using these structural characteristics.

Scattering model for tetrapod can be inspired by scattering model for cylinder because the tetrapod is regarded as the assembly of four cylinder. The position vectors of cylinder are decomposed into a longitudinal and a transverse element in cylindrical coordinate system (Figure 2.1). The amplitude of scatted light is deduced by production of a longitudinal and a transverse element after volume integration. And its square becomes the From Factor after performing the average for the all solid angle.

However, this cylinder model cannot describe the scattering intensity of tetrapod because the rotation about the direction vector of every angular coordinate cannot be considered whereas the rotation by polar angle and azimuthal angle can be considered (Figure2.2).

In this study, modified cylinder model which can consider the rotation about the direction vector of every angular coordinate was presented and its validity was verified. Using this model and the regularity of tetrapod, the scattering model for tetrapod was also presented. Scattering intensity and pair distance distributions are materialized by numerical calculation of presented model and it was confirmed that this model describes the geometry of tetrapod properly. Experimental scattering intensity of well-defined tetrapod nanoparticles which was synthesized by continuous precursor injection method was measured by SAXS experiment and the results comparing experimental data with this model are also presented.

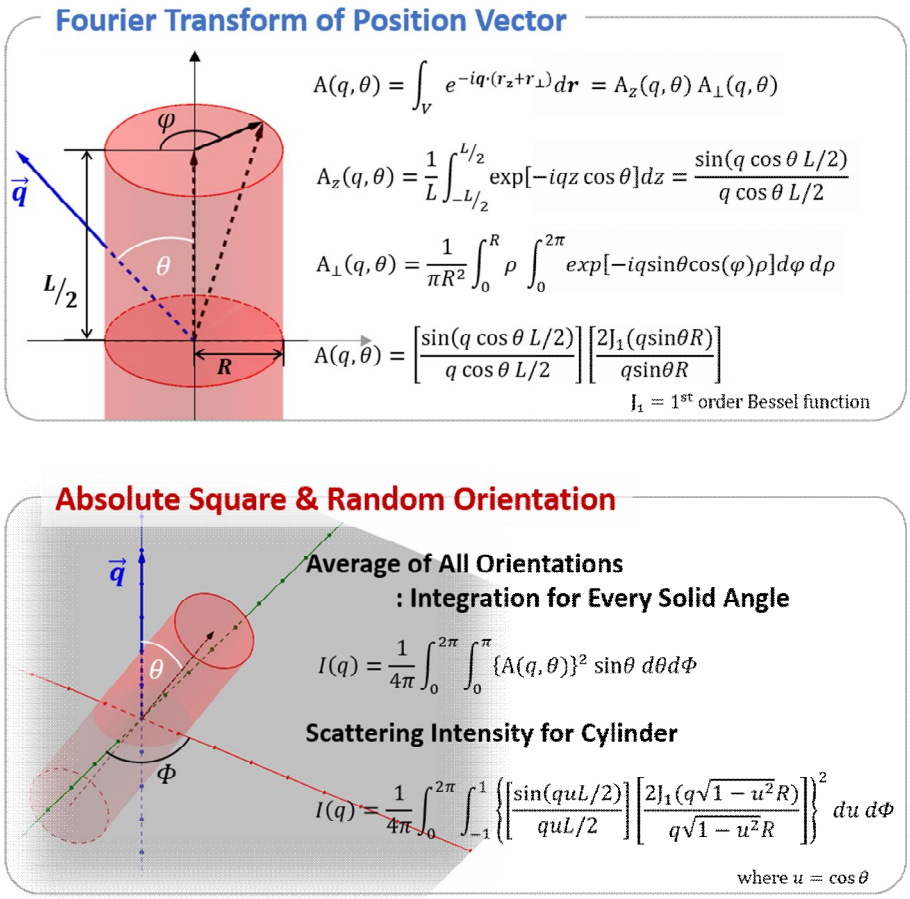

Figure 2.1 Position vectors of scattering model for cylinder. The longitudinal and transverse element of position vector in cylindrical coordinate system and spherical coordination system for consideration of random orientation.

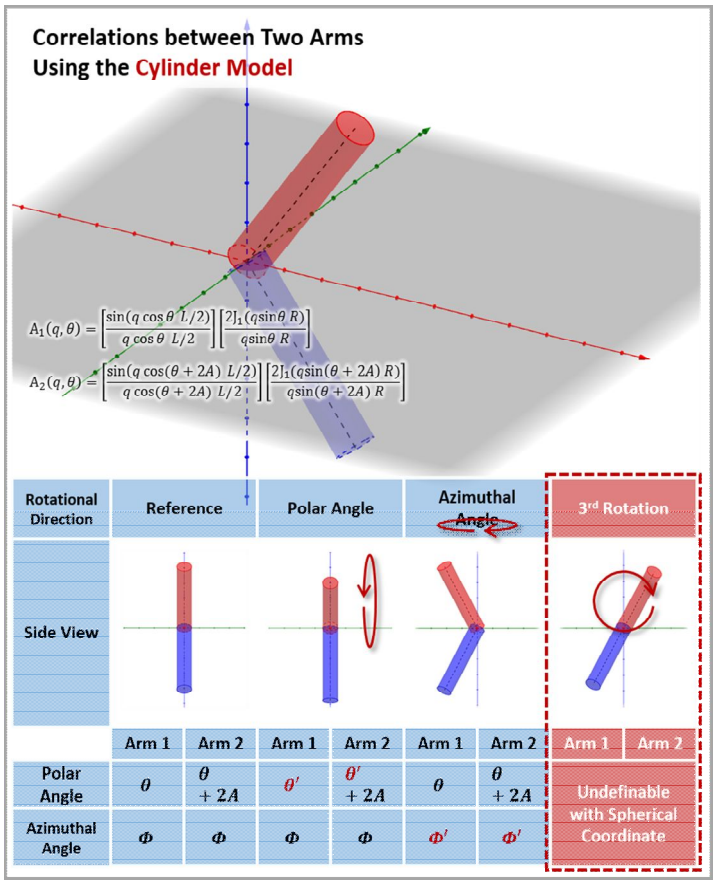

Figure 2.2 Scattering model for cylinder. When there are two arms, cylinder model can not consider the scattering intensity from the 3rd rotation.

2.2. Scattering model for Tetrapod with Cylindrical Arms

2.2.1 Modified-Scattering Model for Cylinder

As above mentioned, the typical scattering model for cylinder cannot consider the random orientation of tetrapod. However, due to having same geometry, we can refer how to express the position vector and consider the random orientation, except rotation at every angular coordination.

The light scattered from the scattering center experience the constructive interference when the path differences of scattered light were the integer of wave length whereas the destructive interference is occurred when the path differences were not integer of wave length. Therefore, the amplitude of light scattering is deduced by Fourier transformation of position vectors which represent the geometry of certain objects with scattering vector, which is given by

$$A(\boldsymbol{q}) = \int_V e^{-i\boldsymbol{q}\cdot\boldsymbol{r}} d\boldsymbol{r} \qquad (1)$$

The position vectors of cylinder can be decomposed into a longitudinal elements and a transverse elements in cylindrical coordinate system.

Therefore the scattering amplitude for the cylinder which is oriented at an angle(θ) from the scattering vector(Figure 2.2) is the product of both contributions[4](Guinier and Fournet, 1955). The reason why the θ is presented in this model is for the mathematical convenience by fixing the scattering vector to the polar axis and varying the θ.

$$A(q,u) = \int_V e^{-iq\cdot(r_z+r_\perp)} d\boldsymbol{r} = A_z(q,u)\, A_\perp(q,u) \tag{2}$$

$$A_z(q,u) = \frac{1}{L}\int_{-L/2}^{L/2} \exp[-iquz]dz = \frac{\sin(quL/2)}{quL/2} \tag{3}$$

$$A_\perp(q,u) = \frac{1}{\pi R^2}\int_0^R \rho \int_0^{2\pi} exp\left[-iq\sqrt{1-u^2}\cos(\varphi)\rho\right] d\varphi\, d\rho = \frac{2J_1(q\sqrt{1-u^2}R)}{q\sqrt{1-u^2}R} \tag{4}$$

$$A(q,u) = \left[\frac{\sin(quL/2)}{quL/2}\right]\left[\frac{2J_1(q\sqrt{1-u^2}R)}{q\sqrt{1-u^2}R}\right] \tag{5}$$

where $u=cos\,\Theta$ and J_1 is the first order Bessel function of the first kind.

And then, the scattering intensity is produced by square of amplitude followed by integration for all angular coordination of spherical coordination.

So far, the scattering intensity of cylinder is derivated, and this model has to be modified for being applied to tetrapod because of considering the random orientation.

For the rotational movement, the degree of freedom (DOF) is 3 in three dimensional space. Therefore, in order to consider the random orientation, which is the average of all orientation, at least three rotational directions should be considered. However, if the object has rotational symmetry with respect to any angle, also known as axisymmetry, DOF is decreased by the number of axisymmetry(i.e. spheres : DOF=0 , cylinders : DOF=2. In the scattering model for cylinder above, only two rotational movement are considerd for random orientation. But, because the tetrapod has no axisymmetry, two rotations in cylinder model is not enough to consider the random orientation of tetrapod but needs consideration of additional third rotation.

The two kinds of rotations are correspond to the polar angle

(Θ) and azimuthal angle (Φ), just like cylinder model. And the third one is the rotation about the direction vector of angular coordinate (Θ, Φ) of spherical coordinate system, by the cylindrical angular coordinate (α) (Figure2.3). The direction vector of a bisector of the angle between two arms of tetrapod is suitable for angular coordinate (Θ, Φ) of spherical coordinate system because the tetrapod has 3 x 2 fold rotational symmetricity. Finally, the orientations of four arms can be presented by Θ, Φ and α in three dimensional space.

Figure 2.4 is the example for presenting the orientation of cylinder with this method. At the certain orientation(θ, Φ, α), the dot product of the scattering vector(q) and the position vector(r) which is represent the longitudinal element of an cylindrical arm of tetrapod is equal to the vertical element of the position vector r. And it is found that this vertical element of position vector r is figured to r (cosA cosΘ + sinA sinΘ cosα) from the side view (Figure 2.4−b), which can be deduced that the angle between the scattering vector and the vector r is arccos(cosA cosΘ + sinA sinΘ cosα). Therefor the u in eq.6 would be replaced by cosA cosΘ + sinA sinΘ cosα for the longitudinal contribution of the arm because the u is the cosine function of included angle. But the transverse contribution, however, cannot be figured out with the same way of longitudinal contribution because the angle of φ in eq.5 varying with the angle of α, and besides the φ cannot be expressed by the angle of α.

However, nevertheless, eq.5 can be used for the transverse contribution of arms by replacing u to cosA cosΘ + sinA sinΘ cosα, like as the longitudinal contribution, because the dot products of cylinders oriented at vector r and r' with the scattering vector are exactly same. It means that there exist the orientation of (Θ', Φ, α=n π/2) which have the same vertical element with the orientation of (Θ, Φ, α≒n π/2), therefore the average of all orientation from a single arm does not change. All after, the amplitudes of scattered light from each arm of tetrapod are given by

$$A_n(q,\theta,\alpha) = \left[\frac{\sin(qu_nL/2)}{qu_nL/2}\right]\left[\frac{2J_1(q\sqrt{1-u_n{}^2}R)}{q\sqrt{1-u_n{}^2}R}\right] \tag{6}$$

$$u_1 = \cos A\cos\theta + \sin A\sin\theta\cos\alpha$$

$$\begin{aligned} u_2 &= \cos A\cos(\theta+\pi) + \sin A\sin(\theta+\pi)\cos\left(-\alpha+\frac{\pi}{2}\right) \\ &= -\cos A\cos\theta - \sin A\sin\theta\sin\alpha \end{aligned}$$

$$\begin{aligned} u_3 &= \cos A\cos\theta + \sin A\sin\theta\cos(\alpha+\pi) \\ &= \cos A\cos\theta - \sin A\sin\theta\cos\alpha \end{aligned}$$

$$\begin{aligned} u_4 &= \cos A\cos(\theta+\pi) + \sin A\sin(\theta+\pi)\cos\left(-\alpha+\frac{3\pi}{2}\right) \\ &= -\cos A\cos\theta + \sin A\sin\theta\sin\alpha \end{aligned} \tag{7}$$

where the negative in front of α is respect to rotational direction. The arm number 1 and 3 rotate by opposite direction with the arm number 2 and 4. Numbers of arm are assigned by clockwise from the top view.

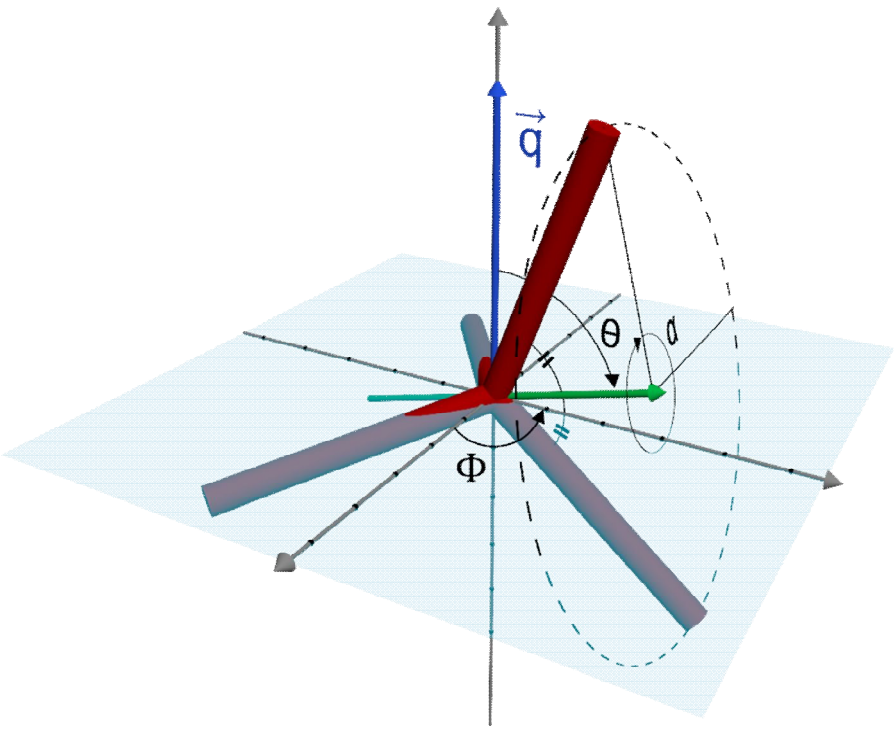

Figure 2.3 The rotational directions of tetrapod for random orientation. The bisector(green allow) is the axis of additional rotation(α)

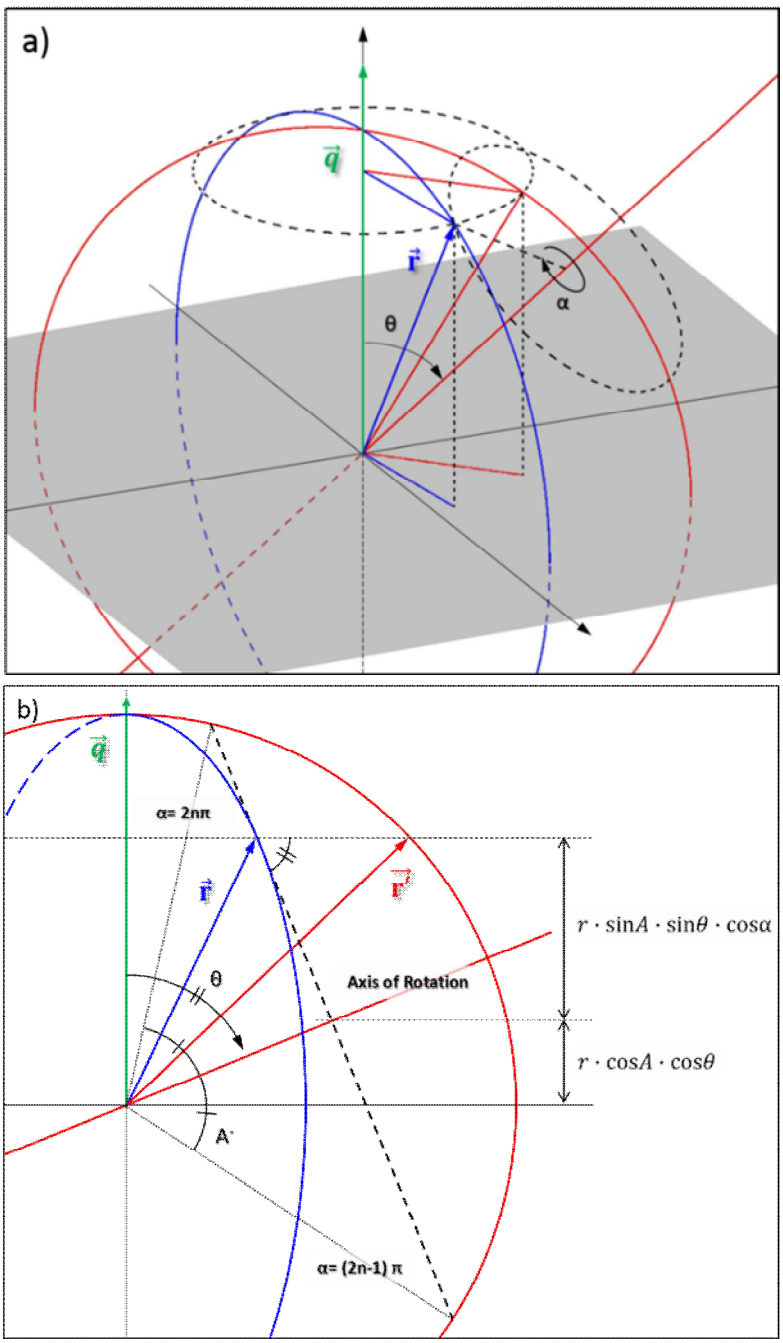
a)
$\vec{q}$
$\vec{r}$
θ
α
b)
$\vec{q}$
α= 2nπ
$\vec{r}$
$\vec{r}'$
θ
Axis of Rotation
A
α= (2n-1) π
$r \cdot \sin A \cdot \sin\theta \cdot \cos\alpha$
$r \cdot \cos A \cdot \cos\theta$

Figure 2.4 The vector(r) for longitudinal element of an arm oriented at (θ, Φ, α). The same colors belong to the same plane. b) is the view of a) from normal to red plane. An angle of A is the half of tetrahedral angle(=109.5/2 °)

2.2.2 Form Factor of Tetrapod

From the Debye scattering formula, the scattering amplitude of object assembly is simple sum of amplitudes from each object. Therefore, assuming a tetrapod is the assembly of four arms, the amplitude of scattered light from a single tetrapod is found by sum of amplitude from each arm, and its square becomes the scattering intensity of a single tetrapod, which is Form factor of tetrapod (eq.8). It can be split base on n=m or not into two terms(eq.2), and the first term represents the scattering intensities from individual arms and the second term is the scattering intensity originated from the correlations between pair of arms[6].

$$A(q) = \sum_{n=1}^{4} A_n(q) \cdot e^{-iqr_n} \tag{8}$$

$$\begin{aligned} I(q) &= \langle |A(q)||A^*(q)| \rangle \\ &= \sum_{n=1}^{4} \langle A_n(q) \cdot A_n^*(q) \rangle + \left\langle \sum_{n=1}^{4} \sum_{m \neq n}^{4} A_n(q) \cdot A_m^*(q) \cdot e^{-iqr_{nm}} \right\rangle \end{aligned} \tag{9}$$

where angle bracket of eq.9 stands for the random orientation, which is the average of all orientations. The scattering amplitudes and intensities from each arm and correlation are not identical because of different orientation and relative position although all arms have same dimensions and included angles. However, considering the random orientation, the scattering intensity from same geometric structures should be identical. Therefore the correlations from each pair of arms also should show same scattering profiles because all of six pairs are isomorphic. Therefore, the scattering intensity of tetrapod is simplified and is given by

$$I(q) = 4 \times I_{\mathrm{arm}}(q) + 6 \times I_{\mathrm{Corr}}(q) \tag{10}$$

The second term of eq.9 is the scattering intensity from the correlation of any pair of arms and it can be expanded as

$$\left\langle \mathrm{A_m}(q,\theta,\alpha) \cdot \mathrm{A}_n^*(q,\theta,\alpha) \cdot e^{-\mathrm{iqr}_{mn}} \right\rangle + \left\langle \mathrm{A}_n(q,\theta,\alpha) \cdot \mathrm{A}_m^*(q,\theta,\alpha) \cdot e^{-\mathrm{iqr}_{nm}} \right\rangle \tag{11}$$

where the vector r represents the origin of arms position. In order to make the tetrapod with cylinders, the direction of the vector r should be same with u and its magnitude is L/2 (Figure 2.5).

Because the amplitudes of scattered light form arms of tetrapod are the real functions, conjugate complexes of the amplitude from the correlations is same with original one. Therefore, the scattering intensity from the correlations can be simplified to cosine function.

$$\begin{aligned}
&\left\langle \mathrm{A_m}(q,\theta,\alpha) \cdot \mathrm{A}_n^*(q,\theta,\alpha) \cdot e^{-\mathrm{iqr}_{mn}} \right\rangle + \left\langle \mathrm{A}_n(q,\theta,\alpha) \cdot \mathrm{A}_m^*(q,\theta,\alpha) \cdot e^{-\mathrm{iqr}_{nm}} \right\rangle \\
&\quad = 2\left\langle \mathrm{A_m}(q,\theta,\alpha) \cdot \mathrm{A}_n(q,\theta,\alpha) \cdot \left(\frac{e^{-\mathrm{iqr}_{mn}} + e^{\mathrm{iqr}_{mn}}}{2} \right) \right\rangle \\
&\quad = 2\left\langle \mathrm{A_m}(q,\theta,\alpha) \cdot \mathrm{A}_n(q,\theta,\alpha) \cdot \cos(q \cdot {}^{L}/_{2} \cdot (u_m - u_n)) \right\rangle
\end{aligned} \tag{12}$$

By putting the eq.6 and 12 into eq.10, the scattering intensity from tetrapod which is the Form Factor of tetrapod is presented by eq13 (where n, m=1~4, n≠m).

$$I(q) = \frac{1}{\pi^2}\int_0^{2\pi}\int_0^{\pi}\int_0^{\pi}\left\{\left[\frac{\sin(qu_n L/2)}{qu_n L/2}\right]\left[\frac{2J_1\left(q\sqrt{1-u_n{}^2}R\right)}{q\sqrt{1-u_n{}^2}R}\right]\right\}^2 \sin\theta\, d\alpha\, d\theta\, d\phi$$

$$+\frac{3}{\pi^2}\int_0^{2\pi}\int_0^{\pi}\int_0^{\pi}\left[\frac{\sin(qu_m L/2)}{qu_m L/2}\right]\left[\frac{\sin(qu_n L/2)}{qu_n L/2}\right]$$

$$\times\left[\frac{2J_1(q\sqrt{1-u_m{}^2}R)}{q\sqrt{1-u_m{}^2}R}\right]\left[\frac{2J_1(q\sqrt{1-u_n{}^2}R)}{q\sqrt{1-u_n{}^2}R}\right]\cos\left(q(u_m-u_n)\cdot {}^{L}/_{2}\right)\sin\theta\, d\alpha\, d\theta\, d\varphi \qquad (13)$$

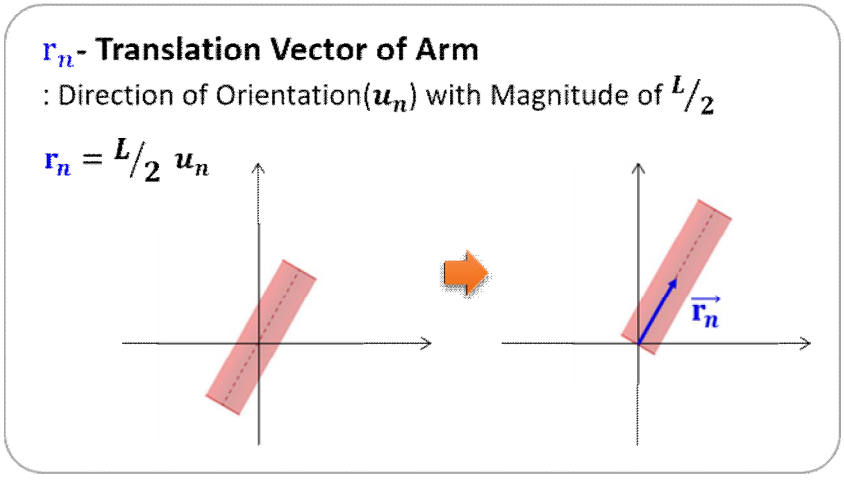

Figure 2.5 Translation vector of cylindrical arm of tetrapod : the orientation of the vector is same with u and magnitude is L/2.

2.3. Result & discussion

2.3.1 Validity of Modified Scattering Model for Cylinder

The scattering model for cylinder was modified by adding the rotation about direction vector of angular coordinate for consideration of random orientation of tetrapod. Nonetheless, the scattering intensity from a single arm or cylinder should not change because the added rotation does not make the change of volume. Therefore both scattering intensity functions from scattering model for cylinder and its modified one should be same.

However, it is very hard to demonstrate that scattering intensity functions from cylinder model and arm of tetrapod model are identical mathematically because the angle of α is inside the first order Bessel function which is at the denominator.

Therefore, in order to compare the scattering intensity profiles from an arm of tetrapod(with α) and a cylinder(without α), we used the numerical calculation method. The results of numerical calculation show that all scatting profiles from the cylinder model and the arm of tetrapod model are exactly same (Figure2.6).

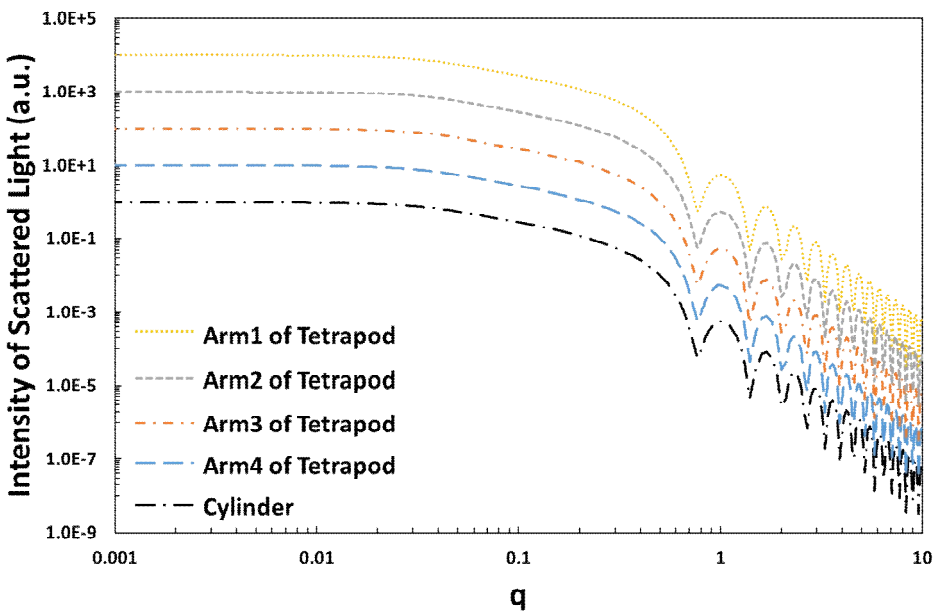

Figure 2.6 The scattering intensity profiles from each arm of tetrapod and a cylinder with same dimension (L=100, R=5).

2.3.2 Scattering intensity and PDDF of the Scattering Model for Tetrapod

Figure 2.7 is the scattering intensity profiles and the Pair Distance Distribution Functions of tetrapod which is also results by numerical calculation. Since the total scattering intensity of tetrapod is obtained by summation of the intensities from each arm and correlation, the scattering profile of tetrapod should have the characteristics of both curves.

Because the scattering profile of tetrapod is almost same with the profile of cylinder and corresponds to cylindrical arm at the above the plateau region, therefore, it can be presumed that the shoulder developed at the entrance of plateau comes from the scattering intensity from correlations between arms. The fact that positions of shoulder do not change by the radius but by the length of arm support this hypothesis.

The small plateau region just after the shoulder is not the Guinier region of cylinder, which is came from lower q range, but the first fringe of scattering intensity profile from correlations. After that, however, scattering intensity from correlations is decreased rapidly and do not affect total scattering intensity.

Though it is possible to find the difference with the scattering models by the comparing the scattering intensity profiles and to estimate the reason why, these series of steps is not easy to accept because it is not visual. However, the pair distance distribution function which is a kind of histogram of distance

between scattering centers can allow the estimation of geometry of object visually.

The pair distance distribution function of tetrapod is the accumulation of the pair distance distribution functions of arms and its correlations (Figure 2.8). For the pair distance distribution function of cylinder, there comes a peak for the radial distance and straight line for the vertical distance of cylinder body in sequence. For the correlation, as population of distance between two lines with certain angle, the pair distance distribution function is increased until the length of line and deceased up to the maximum distance between two lines. The pair distance distribution function of tetrapod has the features of cylinder and correlation, and describes the structural property of tetrapod.

The pair distance distribution function of tetrapod is obtained by numerical calculation and interpreted using pair distance distribution function of cylinder and its correlation which is well-known, we verify the result of pair distance distribution function of tetrapod using simple simulation software, which can provide the distance distribution of assigned coordinates. Figure 2.9 show the object model and its result of simulation. The pair distance distribution function from simulation shows profiles having same characteristics with the pair distance distribution function of scattering model for tetrapod.

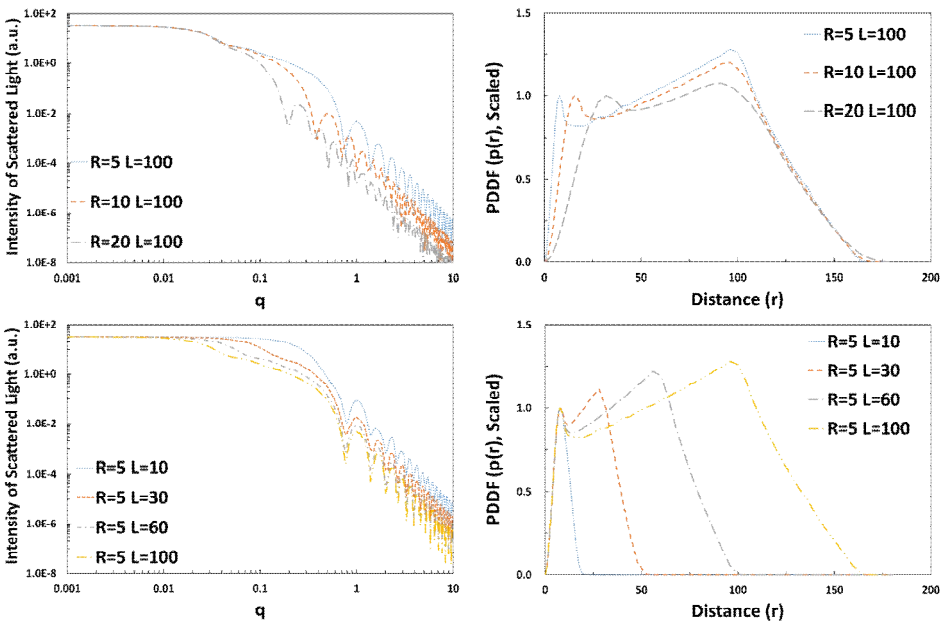

Figure 2.7 The scattering intensity profiles and PDDFs of tetrapods with varying radius and length.

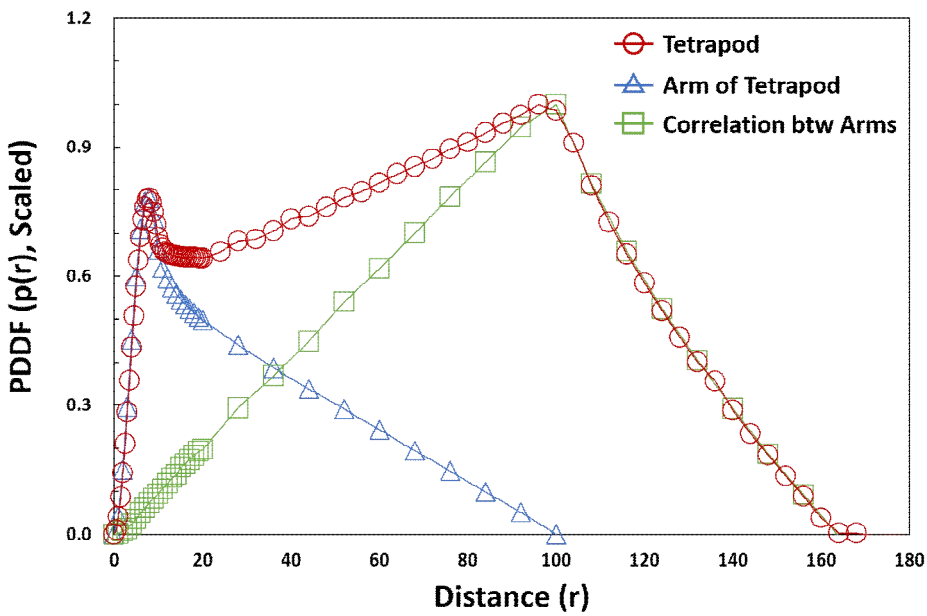

Figure 2.8 The pair distance distribution function of tetrapod(red), cylinder(blue) and correlation(green) with R=5, L=100.

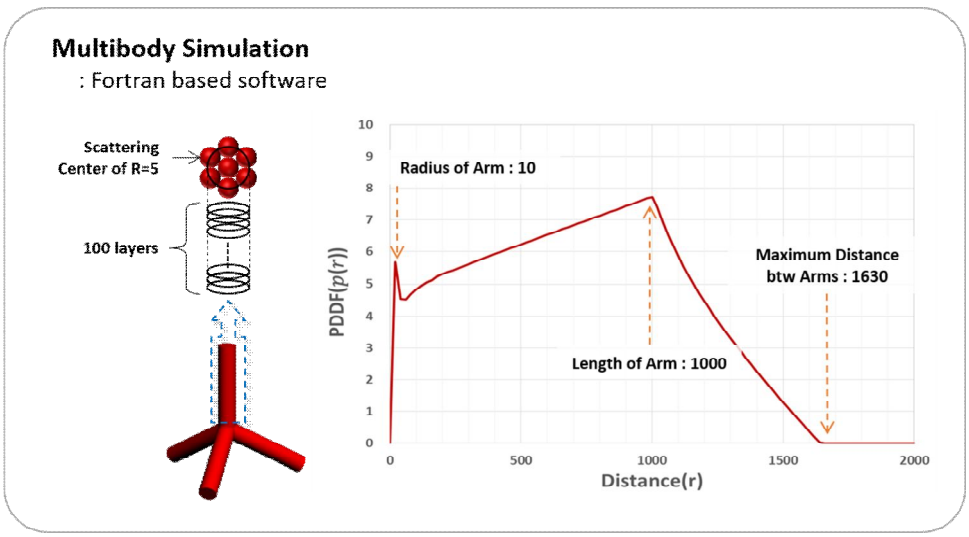

Figure 2.9 The simulation results for pair distance distribution function of tetrapod.

2.3.4 Model Expansion to Regular Multi-pod

In this study, we demonstrate that scattering functions of tetrapod with identical arms and include angles can be established even though it is an anisotropic structure. Likewise, scattering function of multipod structure with identical arms and include angles can be established by similar manner. The only thing to consider is that there would be more than one kind of angle according to the combination of arms and corresponding correlations.

For example, octapod[7] [8] [9], which is multipod with eight arms connecting the centroid of a regular hexahedron to its vertices, has 28 combinations of two arms. Among them, 12 combinations with neighboring arms have an angle of 70.5°, other 12 combinations with face diagonal arms have an angle of 109.5° and the other 4 combinations with space diagonal arms have an angle of 180°. As the rotation about line connecting the center of top and bottom faces of hexahedron, all orientations can be covered by three kinds of correlations. Therefore the scattering amplitude from multipod with eight arms is determined by the scattering amplitude of arm and the three kinds of correlations. Likewise, the hexapod, which is formed by connecting the centroid of an octahedron to its vertices, can be described by two kind of correlations (90, 180).

Thus, for the anisotropic multipods with rotational symmetry,

the position of arms would be described by rotation about symmetry axis and scattering intensity can be obtained by considering the kinds of included angles.

Note that the overlapped volume around the centroid is disregarded in this model. For tetrapod, due to the large included angle, overlapped volume is so small that it does not affect total scattering intensity. However, it is impossible to disregard the overlapped volume if the length of arms is too short compared with the radius or the angles between arms are decrease due to increase of the number of arms. In this case, the appropriate object should be placed and all amplitudes are considered individually.

2.4. Conclusion

The scattering model for anisotropic tetrapod is presented. In order to consider the random orientation of anisotropic tetrapod, the additional rotation about axis of rotational symmetry was introduced. By numerical calculation, the scattering intensity profile and the pair distance distribution function of tetrapod was presented and showed that the presented model describes the geometry of tetrapod successfully

Furthermore, the small angle x-ray scattering experiment was performed for tetrapod nanoparticles and its results are compared with scattering model. In order to obtain the form factor of tetrapod experimentally, SAXS for dilute concentration (0.1mg/ml) was measured and specified by comparing with higher concentrations. Not only the scattering intensity but also the pair distance distribution function which is reduced by inverse Fourier transform method were compared with model. Consequently, though there was slight difference at high q range, overall profile of the scattering intensity profile and the pair distance distribution function from SAXS show the characteristics of tetrapod and were well fitted to the models. From these results, we demonstrate that the presented scattering model is acceptable for tetrapod.

The way of approach for scattering model of tetrapod is applicable to multipod formed by connecting the centroid to its vertices. Increasing a number of arms merely would complicate

the calculations because of increasing the correlations to consider.

2.5. References

(1) Jaehoon Lim, Kookheon Char Chem. Mater. 2013, 25, 1443-1449.

(2) Carsten Svaneborg and Jan Skov Pedersen, THE JOURNAL OF CHEMICAL PHYSICS, 2012 136, 104105.

(3) Carsten Svaneborg and Jan Skov Pedersen, THE JOURNAL OF CHEMICAL PHYSICS, 2012, 136, 154907.

(4) Guinier & Fournet, Small Angle X-Ray Scattering, (1955)

(5) J.S. Pedersen, Adv. Colloid Interface Sci. 70 (1997) 171-210

(6) R. J. Roe, Methods of X-Ray and Neutron Scattering in Polymer Science, Oxford University Press, 2000.

(7) Z. Zhao, Z. Zhou, J. Bao, Z. Wang, J. Hu, X. Chi, K. Ni, R. Wang, X. Chen, Z. Chen and J. Gao, NATURE COMMUNICATIONS, 2013, 4, Article number: 2266

(8) K. Miszta, J. de Graaf, G. Bertoni, D. Dorfs, R. Brescia, S. Marras, L. Ceseracciu, R. Cingolani, R. van Roij, M. Dijkstra and L. Manna, NATURE MATERIALS, 2011, 10, 872

(9) E. Conca, M. Aresti, M. Saba, M. F. Casula, F. Quochi, G. Mula, D. Loche, M. R. Kim, L. Manna, A. Corrias, A. Mura and G. Bongiovanni, Nanoscale, 2014, 6, 2238

Chapter 3. Characterization of Dispersion Structure of Tetrapod Nanoparticles using Small Angle X-Ray Scattering

3.1. Introduction

Various inorganic nanoparticles having unique properties differing with bulk state are composite with functional polymers for synergetic effect, which facilitates the processability and functionalities resulted from the interaction with surround materials. For the full development of their distinctive properties, depending on the applications, appropriate dispersion structure of inorganic nanoparticles within polymer matrix is achieved preferentially[1][2][3][4].

In the case of tetrapod nanocrystals, in order to utilize their exceptional optoelectronic properties, homogeneous dispersion structure which maximize the functionality from the interaction with functional polymer matrix is preferred[5]. Meanwhile, heterogeneous structure which locate the tetrapod nanocrystals to certain area is favorable for constructing the bi-continuous path for charge transfer.

Surface modification of inorganic nanoparticles with organic polymers, hybridization, is one of the way to control the dispersion structure of organic/inorganic polymer nanocomposite system[6][7][8][9]. Dispersion structure of surface modified inorganic nanomaterials within organic polymer matrix is determined by the enthalpic interaction as well as entropic interaction between the brush polymers which modify the surface of inorganic materials and matrix polymer. Description of relations between brush polymer and matrix polymer is based on the theoretical analysis from the planar brushes[10][11][12][13], which informs that the areal chain density and the ratio between the molecular weight of brush polymer and matrix polymer determine the features of inter-digitation. For the nanoparticles instead of planar substrate, since the curvature of nanoparticles provides an additional configurational space for both polymer chains, the feature of inter-digitation are affected by curvature, besides molecular weight of both polymer and areal chain density[6][14].

Tetrapod nanocrystals are also able to be induced the homogeneous dispersion structures by hybridization, which enable the full development of their unique properties for the application to the optoelectronics. Zentel et al. reported that hybridized tetrapod nanocrystals with semiconducting block copolymers are dispersed in polymer matrix homogeneously[5]. In this results, they show the dispersion structures of hybrid and bare tetrapod having different arm length using TEM.

Generally, these dispersion structures are characterized by typical microscopic[15] or spectroscopic[16] or photography[17] methods. However, results from these methods are restricted to relatively small area as well as have the lack of representability to

stand for the dispersion structure of the whole sample. Especially for the tetrapod nanocrystals, by typical methods, dispersion structure is harder to be characterized then other shapes of inorganic materials because of their three dimensional anisotropic structure as well as the pointy shape. In the report of Zentel et al[5]. mentioned above, depending on the arm length of tetrapod, there are few cases which is hard to find the distinct difference of dispersity between hybrids and blends only with TEM images.

Therefore, recently researchers have reported their results about controlling the dispersion structure of inorganic nanomaterials with not only typical microscopic and spectroscopic method but also scattering method for complement. Because the scattering method is able to obtain the ensemble average of dispersion structure for the relatively large area, it is brilliant tool for characterization of structural properties of colloidal system[18][19].

Scattering method would stand out for the tetrapod nanocrystals because the tetrapods within the polymer matrix not only is dispersed homogeneously but also construct the three dimensional structures by stacking the arms of tetrapod which is counted as aggregation for typical methods, and then these structures are able to be characterized by scattering method.

In this study, therefore, the dispersion structure of tetrapod nanocrystals are characterized by small angle x-ray scattering (SAXS) experiment. To compare the difference between the homogeneously dispersed and aggregated structure of tetrapod nanocrystals, SAXS experiments are performed for the hybrids and the simple blends case. Scattering intensity from the dilute solution of tetrapod nanocrystals is also measured to obtain the form factor of tetrapod which contain the information of size and

shape of particles, and then structure factors which contain the information of inter particles correlation are deduced by dividing the total scattering intensity with form factor.

3.2. Experimental Section

3.2.1 Synthesis of Tetrapod Nanoparticles and Brush Polymer

Well-defined CdSe tetrapod nanoparticles were synthesized by continuous precursor injection method[20]. Arm length and raidus of tetrapod nanocrystals are measured by TEM analysis. Surface modification of tetrapod nanocrystals were performed by grafting-to approaches. Polystyrene-block-poly(cysteamine methyl disulfide) diblock copolymer for the surface modification of tetrapod nanocrystals was synthesized by reversible addition fragmentation chain transfer (RAFT) polymerization. The molecular weight of polymers are measured by GPC and the additions or substitutions are checked by ^{1}H NMR, ^{19}F NMR and FT-IR. All the tetrapod nanocrystals and Brush polymers are synthesized as described in the literatures[20][21][22].

Synthesis of CdSe Tetrapod Nanoparticles

For the preparation of cadmium oleate ($Cd(OA)_2$) solution, 10 mmol of cadmium oxide (CdO), 7.8 mL of oleic acid (OA), 6.2 mL of 1-octadecene (ODE), and 1 mL of n-trioctylphosphine (TOP) were placed in an 100 mL 3-neck round flask coupled with a condenser. The mixture was heated to 280 ° C under N_2 flow for 20 min. After the mixture was optically clear, the round flask was cooled down to 50 ° C and added 0.14 mmol of

cetyltrimethylammonium bromide (CTAB) under N2 flow. Separately, 12 mmol of Se and 6 mL of TOP were mixed in a 50 mL 2-neck round flask with a condenser and heated at 200 ° C until the mixture became a transparent solution. After the TOPSe was cooled down to room temperature, 5 mL of TOPSe solution was added to the $Cd(OA)_2$ solution, and the mixed solution was stirred for 5 min.

0.5 mmol/mL of $Cd(OA)_2$ solution was prepared by reacting 5 mmol of CdO, 5 mL of OA, and 5 mL of ODE with the same reaction condition described above. Next, 1 mmol of Se and 10 mL of ODE were loaded into a 100 mL 3-neck round flask and heated up to 300 ° C under N2 flow. When the Se/ODE solution become optically clear, 2 mmol of $Cd(OA)_2$ solution (4 mL) was rapidly injected into the solution and reacted at 270 ° C for 15 min. Finally, 6 mL of ODE was added into the seed solution and cooled down to room temperature.

Five milliliters of seed solution, 2.25 mL of OA, 1.5 mL of TOP, 21.25 mL of ODE, and 0.21 mmol of CTAB were placed in a 3-neck round flask with condenser, followed by heating up to 260 ° C. When the temperature reached 260 ° C, 20 mL of injection solution was added into the seed solution with 0.4 mL/min of injection rate for 50 min. To purify the product, 2 mL of chloroform and an excess amount of acetone were added into the resulting solution until the solution became turbid and centrifuged at 3,000 rpm for 5 min. After the centrifugation the supernatant was decanted, and the precipitate was redispersed in organic solvent such as chloroform, toluene, or hexane. The precipitation and redispersion was repeated until the samples were sufficiently purified.

Synthesis of Polystyrene-block-poly(cysteamine methyl disulfide) diblock copolymer (PS-b-CMD) Polymer Brushes

Polystyrene-block-poly(pentafluorophenol acrylate) (PS-b-PPFPA) :

Styrene monomer which was purified, the chain transfer agent

(benzyl dithiobenzoates) and AIBN were mixed together. Three time of freeze−pump−thaw cycles were performed for removing the oxygen within the solution. RAFT Polymerization was carried out at 100 °C under N2 condition. The reaction time and temperatures are adjusted according to desired MW of styrene block. The polymer, macroinitiator for the following polymerization, was purified by precipitation in methanol three times. For introducing the reactive block to the polymer, macroinitiator, AIBN and pentafluorophenol acrylate (PFPA) were dissolved in dry THF. After three times of freeze−pump−thaw cycles, the mixture was stirred under nitrogen at 70 °C for 36 hours, which is also adjusted according to desired MW of PFPA block. The block copolymer of pinkish powder was obtained by precipitation in methanol followed by dried under vacuum at 70 °C for 2 days. The molecular weight and the polydispersity index of block copolymers were measured by gel permeation chromatography (GPC). ^{1}H NMR (300 MHz, CDCl3) : d [ppm] : 7.03 (m), 6.6 (m), 2.21 (m), 1.83 (m), 1.12 (m). ^{19}F NMR (300MHz, CDCl3) : d [ppm] : −163.72 (m), −159.47 (m), −154.41 (m).

Cysteamine methyl disulfide :

Methyl methanethiosulfonate(12g) was dissolved in 80ml of methanol and placed at ice for 1hr. After that, cysteamine hydrochloride(9g) was dissolved in 80ml of methanol, and then the solution added to the methyl methanethiosulfonate solution slowly with stirring under the N2. After remove the ice bath after 1hr, the solution was stirred for 24hrs at room temperature. After that the solvent was evaporated and residual was resolved again in dichloromethane (CH2Cl2) and washed twice with NaOH aqueous solution. Then, the organic upper layer was separated. After drying the oraganic solution with Na2SO4 and removing the solvent, cysteamine methyl disulfide (47%) was obtained by column chromatographic purification. ^{1}H NMR (300 MHz, CDCl3) : d [ppm] : 3.01−3.04 (m), 2.78−2.8 (m), 2.4 (s), 1.38 (br. s).

Polystyrene-block-poly(cysteamine methyl disulfide) :

PS-b-PPFPA and cysteamine methyl disulfide were dissolved in dry THF and stirred under nitrogen at room temperature for 12 hours. Afterwards the solution was precipitated in methanol three times to yield the desired product. ^{1}H NMR (300 MHz, CDCl3) : d [ppm] : 6.9-7.19 (m), 6.6-6.3 (m), 2.4 (m), 1.83 (m), 1.12 (m). ^{19}F NMR (300MHz, CDCl3) : no signals founds. FT-IR : 1020~1250 cm-1 (C-N aliphatic amine vibration), 1545 cm-1, 1690 cm-1 ((O=C-N) stretching vibration), 1250 cm-1 (N-H bending & C-N stretching), 3340 cm-1 (NHCH).

Hybridization of CdSe Tetrapod with PS Brushes in Solution :

CdSe Tetrapod dispersed in THF was mixed with the solution of PS-b-CMD in THF solution. After stirring overnight, the surface of CdSe Tetrapod was functionalized with PS brushes.

Dispersion of Surface Modified Tetrapod Nanocrystals within Polymer Matrix

Surface modified tetrapod nanocrystals and PS-b-CMD block copolymers were dispersed in THF. Frame mold for free standing film are dipping into the solution and then the polynmer film in which tetrapod nanocrystals dispersed. The Thin films thickness were controlled by viscosity and the number of dipping. The films are dried at 60 °C overnight to remove residual solvent. The samples were sliced for TEM analysis after SAXS measurement.

3.2.2 Small Angle X-Ray Scattering Experiment of Tetrapod Nanocrystals

Well-defined CdSe tetrapod nanoparticles whose arm lengths of ~30, ~55 and ~70 nm and radius of 3 nm were prepared by continuous precursor injection method and dispersed in THF for the form factor of tetrapod and in polystyrene homopolymer for blends. For the hybrids, surface modified tetrapod nanocrystals were dispersed in PS-b-CMD diblock copolymer. Because the

range of distance within tetrapod nanoparticles in real space was 6 nm ~ 120 nm, 9A beam line (U-SAXS) of Pohang Accelerator Laboratory which includes the relevant q-range ($0.005 \sim 0.11 A^{-1}$) was used. The scattering data of Energy=11.07 keV and 19.95 keV were merged with minimum deviation in the overlap regions.

SAXS for Form Factor of Tetrapod Nanocrystals

Each tetrapod nanocrystals was dispersed in THF with varying concentration. For the scattering intensity from a single tetrapod, tetrapod nanocrystals were dispersed in solvent of THF with 50dilute concentration (0.1mg-TP/ml-THF) for the exclusion of inter particle correlations. In order to confirm the critical concentration of inter particle correlations, another concentrations (3, 10, 30mg-TP/ml-THF) were prepared.

SAXS for Structure Factor of Tetrapod Nanocrystals for Hybrids and Blends

Scattering intensity from the tetrapod dispersed within polymer matrix was measured with varying concentration (1, 5, 10, 30 wt%) of tetrapod nanocrystals for hybrids and blends. All the tetrapod nanocomposite samples were prepared as free standing films with around 1 mm thickness.

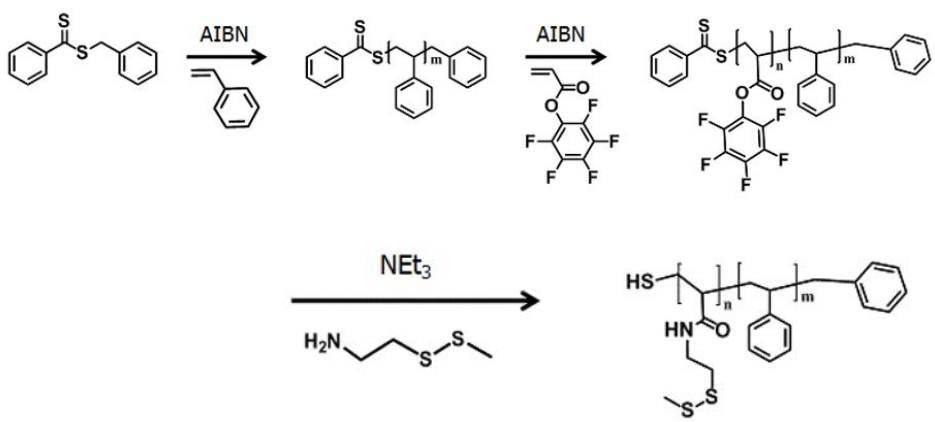

Figure 3.1 Schematic for RAFT polymerization of PS-b-CMD block copolymer for surface modification of tetrapod nanocrystals

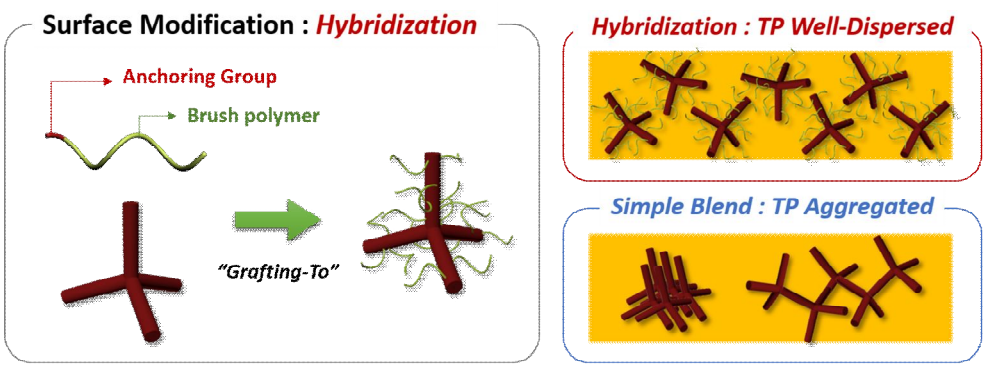

Figure 3.2 Schematic for RAFT polymerization of PS-b-CMD block copolymer for surface modification of tetrapod nanocrystals

3.3. Results and Discussion

3.3.1 SAXS Results of Tetrapod Nanoparticles Dispersed within Solvent

The small angle X-ray scattering experiment was performed for tetrapod solution with different concentrations(0.1mg/ml, 3mg/ml, 10mg/ml(which is only for L=40nm), 30mg/ml). The lowest concentration(0.1,g/ml) was prepared for mimicking the dilute concentration, which has no inter-particle correlations. Technically, scattering from single particle needs infinitely dilute concentration, which is impossible practically. However, if there is no inter-particle correlation effect in relevant q range, the scatting intensity can be treated as form factor.

Scattering intensities from tetrapod dispersed within solvent are presented by Figure 3.3. For the inspection of difference, structure factors were deduced for arm length of 40 nm using the scattering intensity of the lowest concentration as form factor. The blue line in Figure 3.4 is the results from dividing the raw data of the lowest concentration with its binominal smoothing curve, which means the degree of fluctuation of form factor. There are no changes up to 3mg/ml, and from the concentration of 10mg/ml, the signal of inter particle correlation begins to appear at low q range lightly. Therefore the scattering intensity of 0.1mg/ml was used as the form factor of the tetrapod.

The form factors from SAXS experiment were fitted by the

model for tetrapod presented in chapter2 (Figure 3.5). All experiment results were relatively well-fitted to the profiles of scattering model for tetrapod for overall q range except high q. At the high q range, the scattering intensity of SAXS results were higher than the model, we think it come from polydispersity of particles or geometry of arm ends. Because the model assumed that the tetrapods are monodisperse and their arms are the cylinder with plat ends, but the tetrapod nanoparticle cannot be the ideally monodisperse in practical and the real geometry of cylinder end is close to hemisphere or hemiellipsoid.

In order to figure out the difference in real space, the pair distance distribution functions (PDDF) of SAXS results were obtained by Inverse Fourier Transform[23][24][25] (Figure 3.6). It was found that the profiles of PDDF of scattering intensity of SAXS had similar characteristics with PDDF of scattering model for tetrapod. The peaks corresponding to the radius, length were appeared in sequence, and the profiles is finished at the distance corresponding to maximum distance between arms.

However, comparing with model, all these characteristics were a little blurred. The size distribution or the varying radius within an arm caused by hemispherical- or hemiellipsoidal- ends would be the reasons why the characteristics of PDDF curve were blurred. However, since the volume of round ends is much smaller than the total volume of tetrapod, the scattering intensity from end tip is not able to influence to the total scattering intensity. Therefore it was found that the difference only comes from polydispersity of particles, eventually.

3.3.2 SAXS of Results of Tetrapod Nanoparticles Dispersed within Polymer Matrices

The small angle X-ray scattering experiment is performed for tetrapod nanocomposite with different concentrations (30, 10, 5, 1 wt%). Structure factors from each samples were deduced using

form factor of tetrapod from SAXS of tetrapod dispersed within solvent (0.1mg-TP/ml-THF).

Each samples were sliced and analyzed by TEM analysis after SAXS experiment. For the hybrids, tetrapod nanocrystals homogeneously dispersed without any aggregations, while massively aggregate for simple blends(Figure 3.7 and Figure 3.8).

Obviously, the scattering intensity and structure factor of tetrapod nanocomposite for hybrid and simple blend also showed the large difference. In the case of hybrid tetrapod (Figure 3.9), at low concentration, scattering intensity is almost same with form factor of tetrapod, which means that tetrapod were dispersed with in polymer matrix homogeneously, in accordance with the TEM results. However, as increase the concentration of hybrid nanocrystals, the location of the first peak at the low q was shift to higher q region. The peaks (~0.008 A^{-1}) are corresponding to the inter particles distance which is around 800 A in real space. For the highest concentration, the intensity of structure factor was increasing as decreasing the q, while it was never shown for other concentrations. Typically, this trend shows up for non-particular two phase system or phase separations due to the clusters. Because there should be no aggregation due to the hybridization, non-particular two phase due to the connection between arms of other tetrapod were formed. Therefore, it was found that the connected structure are formed at very high concentration, despite the surface of tetrapod nanocrystals are modified with brush polymer. Similarly, intensity of structure factor at high q was also increased with increasing the concentration. q value of this peak at high q region was about 0.08 A^{-1}, which is corresponding to around 8 nm in real dimension, is close to the double of radius of arms, which means that the frequency of arm contact is increase.

On the contrary, scattering intensity of simple blend showed the large difference with the form factor of tetrapod even though concentration of tetrapod was low(Figure 3.10). In the case of hybrids, there was no unusual profiles except the very high concentration. All the structure factors shows the increasing trend

for high and low q region, which mean the 8 and 800 nm were developing at the same time. This structure was able to be described by stacking the arms from different tetrapod nanocrystals.

Meanwhile, in the case of 5 wt% and 10 wt% of simple blend, specific profile or peak whose scattering vector correspond to 40~50 nm was observed in the structure factor. In order to define these peaks, post process for exclusion of cluster and contact of arms was performed (Figure 3.11). Typically, since the increasing trends at low q region was excluded using Lorentzian distribution or Debye Bueche, we removed the cluster peak by Lorentzian distribution. Because the increasing trends at high q was caused by contact of arms, it should follow the Gaussian distribution. Through this post process, the structure factor from the inter particle correlations. The position of peaks was around 0.012 ~ $0.014A^{-1}$, which corresponding to 45 ~ 52 nm in real dimension (Figure 3.12). These distance positioned at the middle of radius and length, and then it should be the distance between arms of other tetrapod nanocrystals. In the TEM images, arms of tetrapod were stacked and tetrapod formed the 5 or 6 membered rings with regularity. Therefore, these peak were originated by the correlations between arms from other tetrapod.

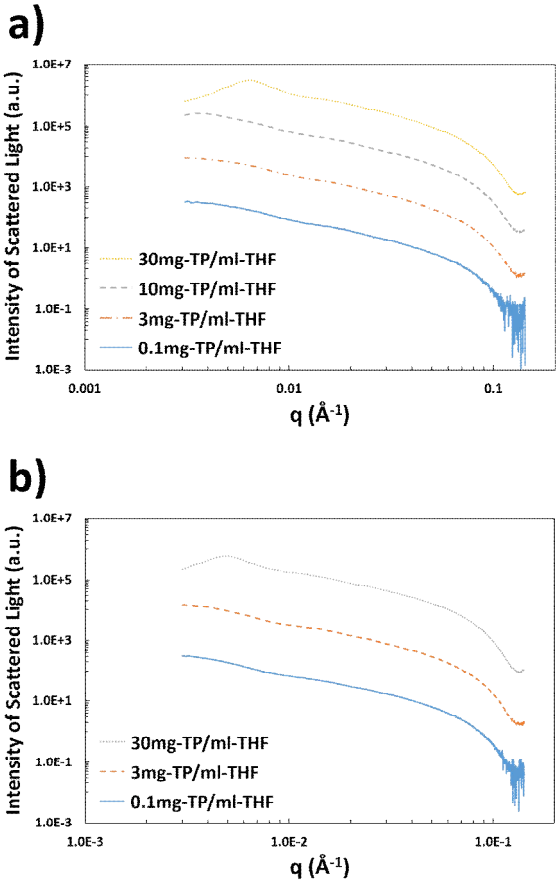
a)
Intensity of Scattered Light (a.u.)
1.0E+7
1.0E+5
1.0E+3
1.0E+1
1.0E-1
1.0E-3
0.001
0.01
0.1
q (Å-1)
30mg-TP/ml-THF
10mg-TP/ml-THF
3mg-TP/ml-THF
0.1mg-TP/ml-THF
b)
Intensity of Scattered Light (a.u.)
1.0E+7
1.0E+5
1.0E+3
1.0E+1
1.0E-1
1.0E-3
1.0E-3
1.0E-2
1.0E-1
q (Å-1)
30mg-TP/ml-THF
3mg-TP/ml-THF
0.1mg-TP/ml-THF

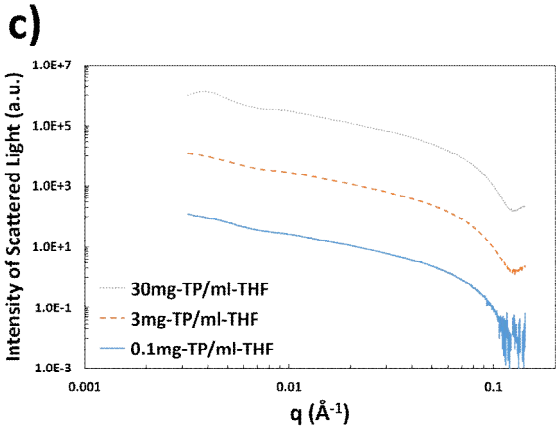

Figure 3.3 Scattering intensity profiles of tetrapod nanopartices with R=~3nm and L=~40nm(a), ~55nm(b) and ~70nm(c)

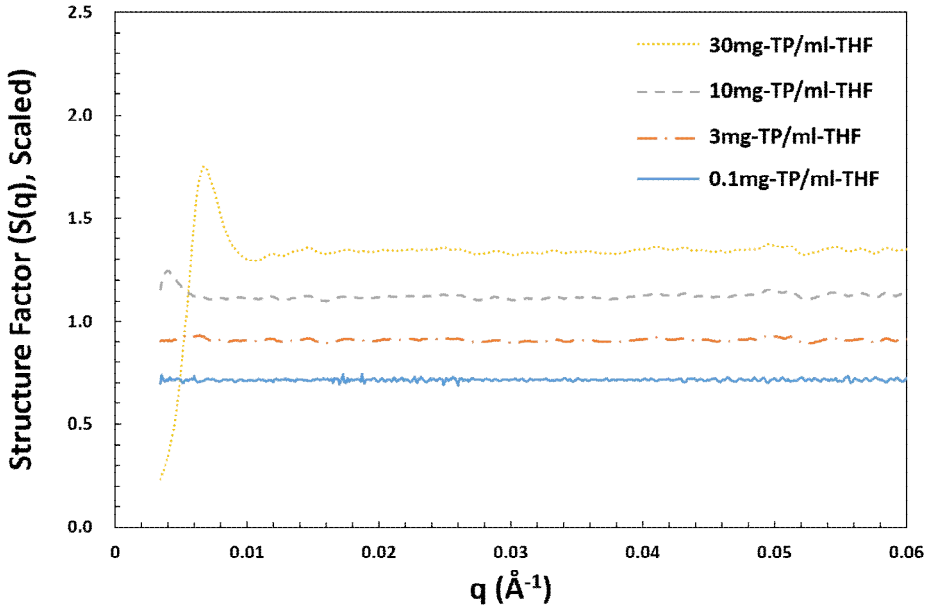

Figure 3.4 The structure factors of tetrapod (L=40) with varying concentration.

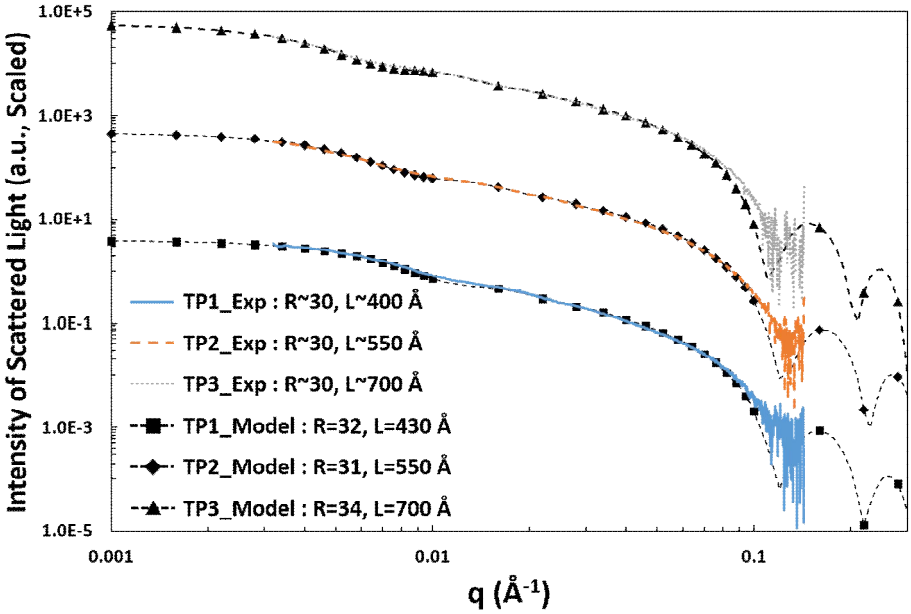

Figure 3.5 The form factors of tetrapod with model fitting

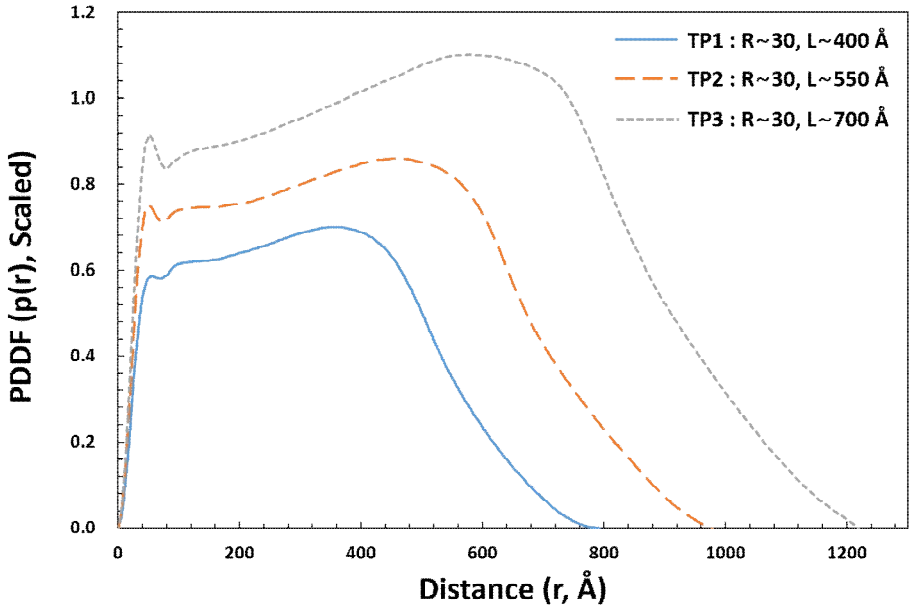

Figure 3.6 Pair Distance Distribution Function of Tetrapod converted by Indirect Fourier Transform

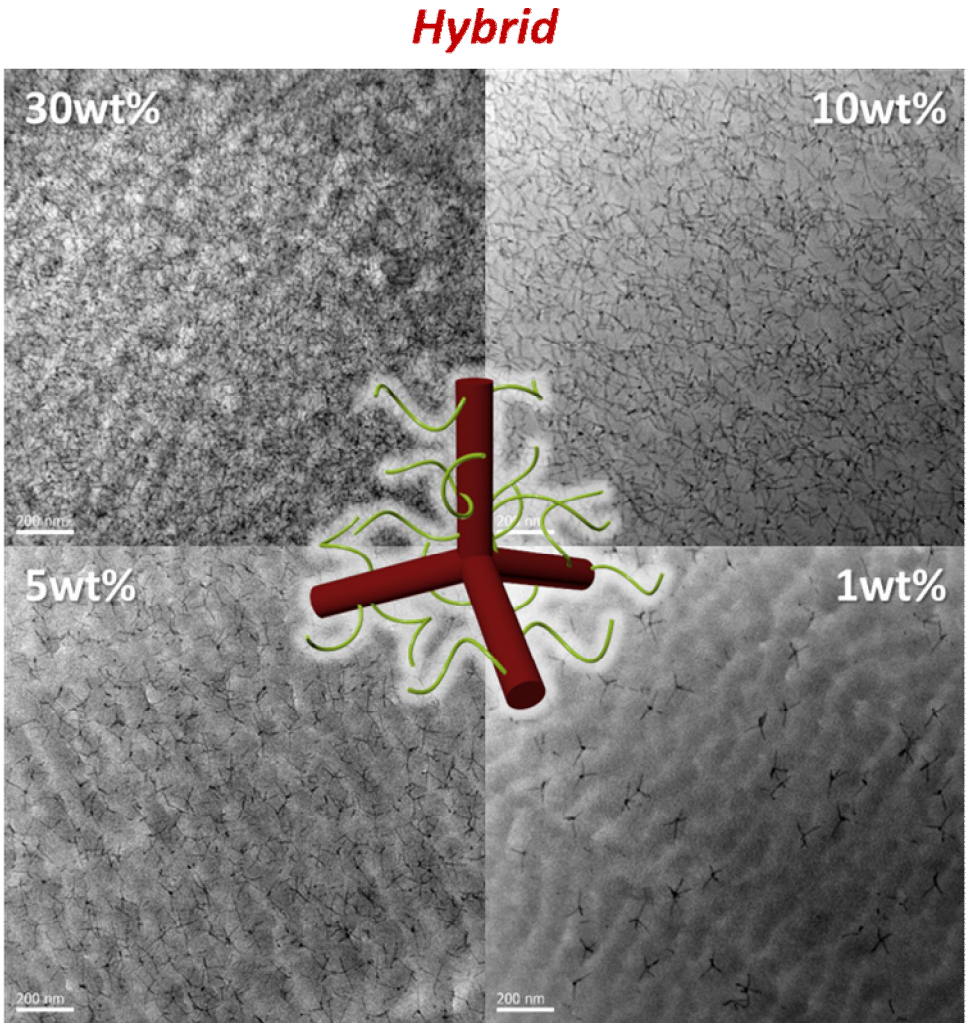

Figure 3.7 Dispersion structure of hybrid tetrapod nanocomposite with varying concentration. TPs are homogeneously dispersed within a polymer matrix.

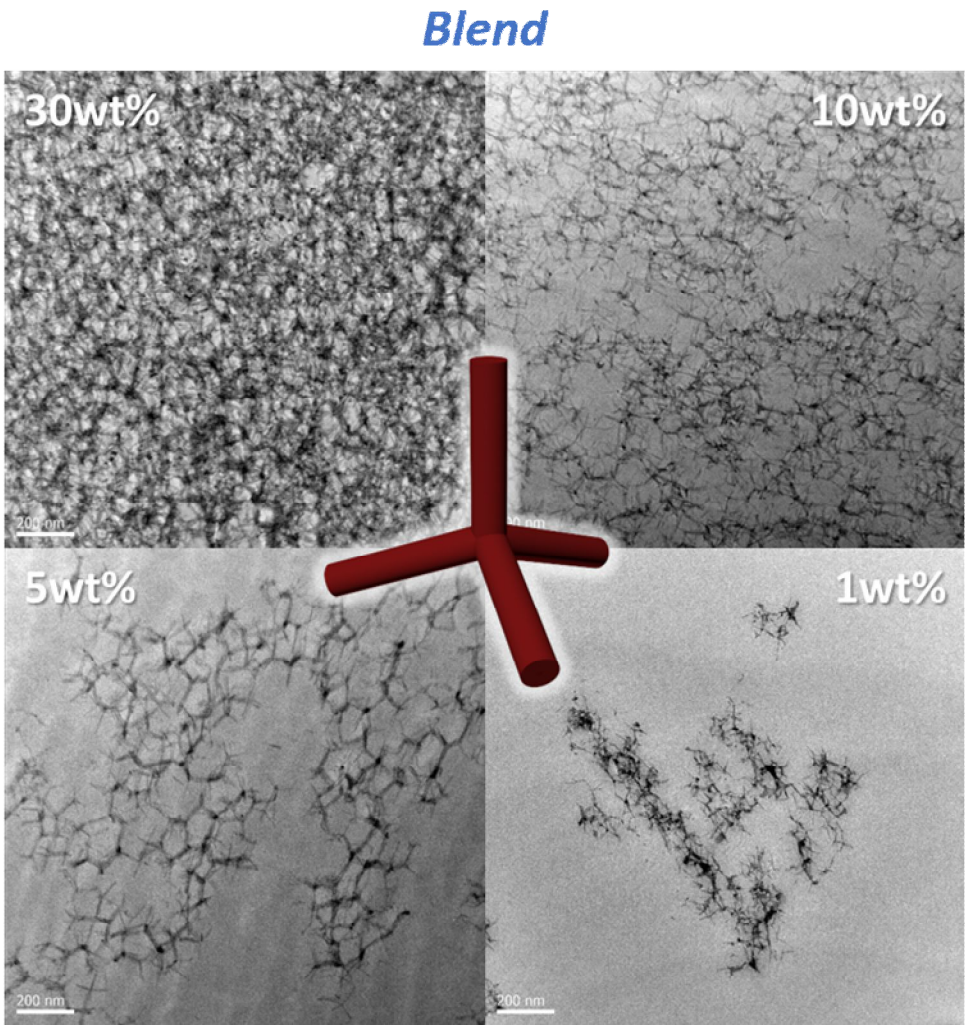

Figure 3.8 Dispersion structure of blend tetrapod nanocomposite with varying concentration. TPs are massively aggregated within a polymer matrix.

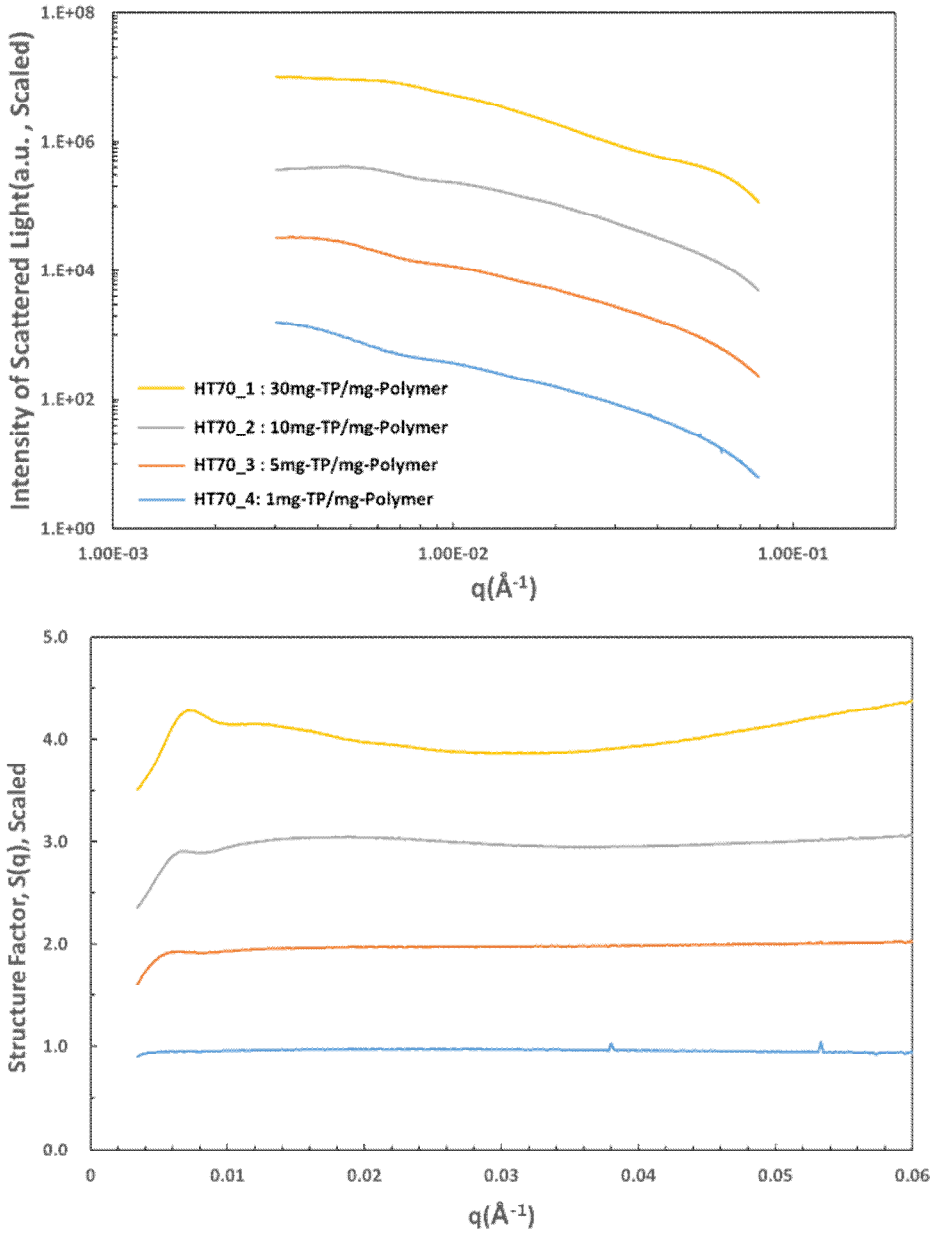

Figure 3.9 Scattering intensity and structure factor of hybrid tetrapod nanocomposite

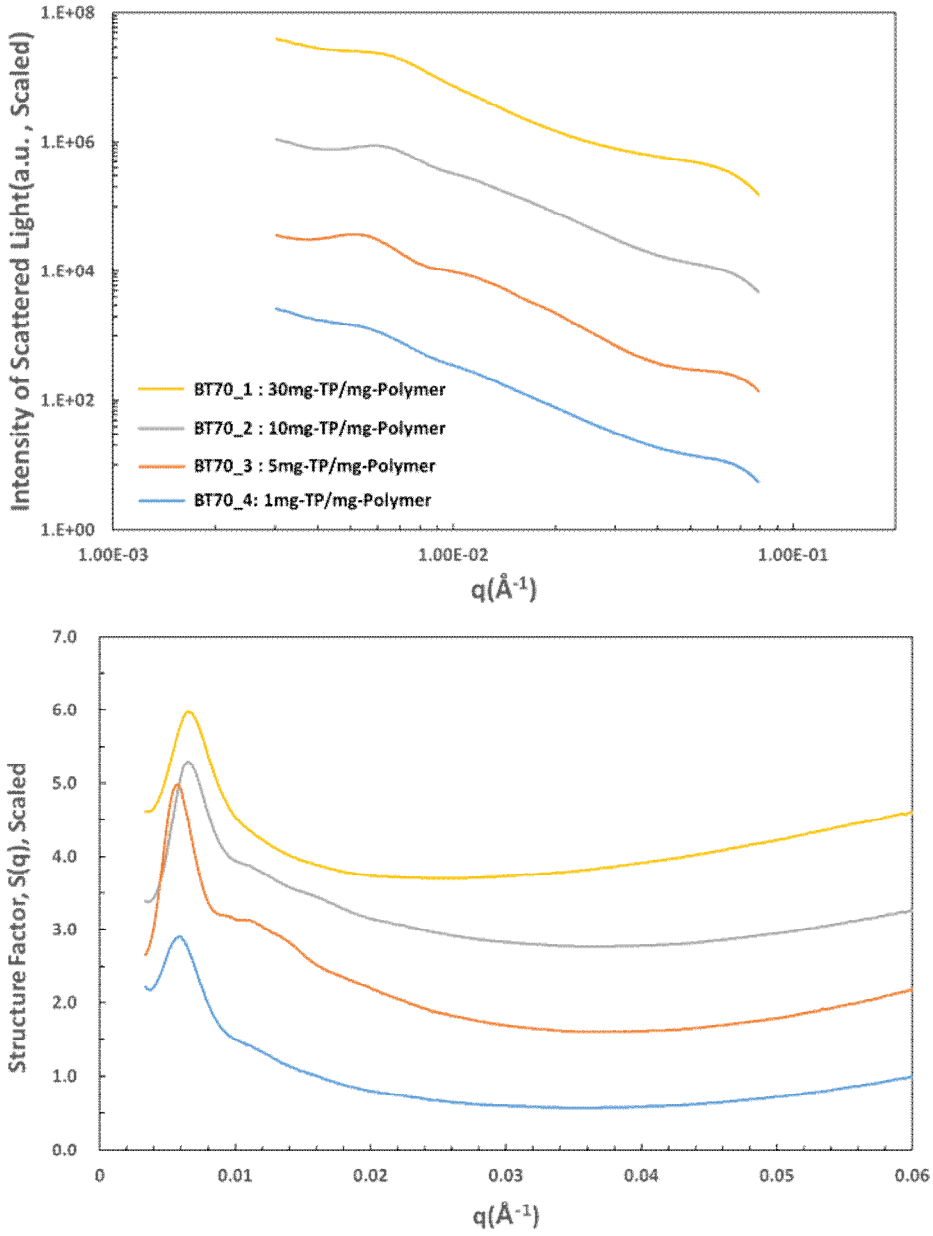

Figure 3.10 Scattering intensity and structure factor of blend tetrapod nanocomposite

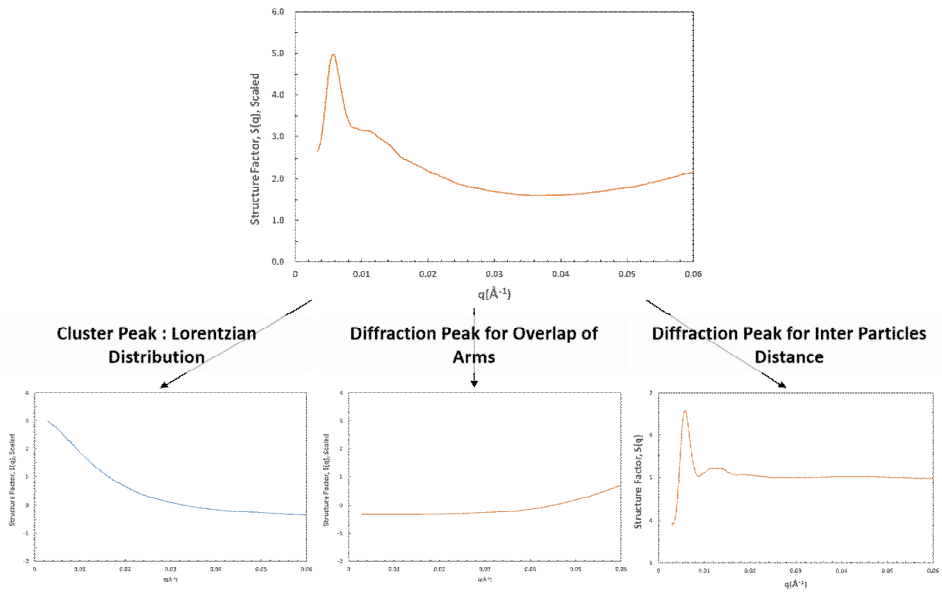

Figure 3.11 schematic for deconvolution of structure factor for blends

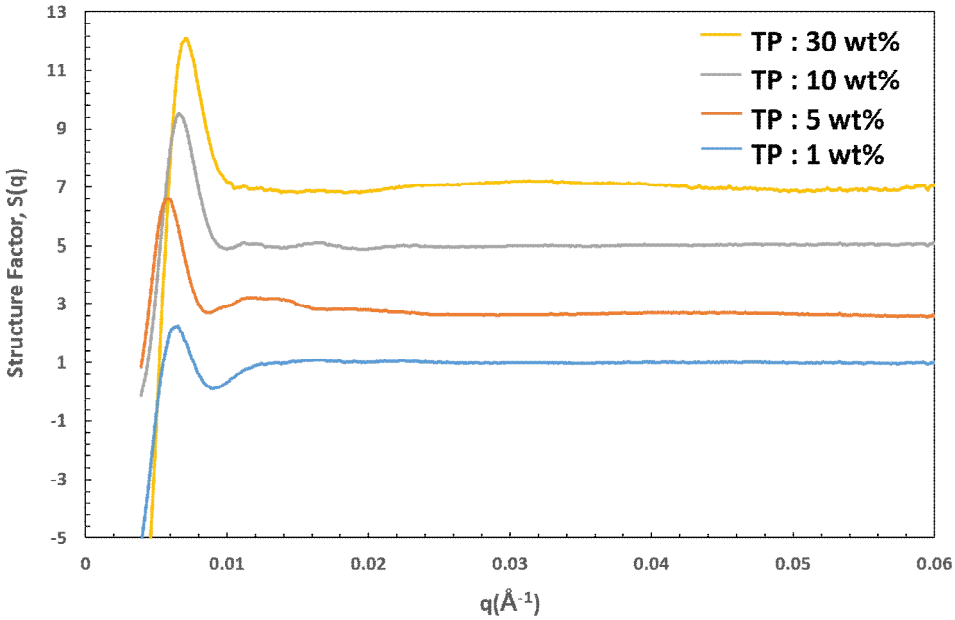

Figure 3.12 Structure factors showing the inter-particle correlations for the blends. After subtracting with the intensities due to the TP clusters at low q and the contact of arms at high q, distinctive scattering peaks for 5 and 10 wt% at 0.012~ 0.014 Å-1 are noted, which correspond to the inter-arm distance (450 ~ 520 Å).

3.4. Conclusion

Dispersion structure of tetrapod nanocrystals were characterized by small angle x-ray scattering experiments.

Form factor of tetrapod nanocrystals was obtained by SAXS experiment for dilute concentration of tetrapod dispersed within solvent. SAXS experiment for the solution varying the concentration of tetrapod were performed for confirmation of critical concentration of dilute concentration. Form factors from SAXS experiments were compared with scattering model for tetrapod. Geometric parameters of tetrapod nanocrystals from model fitting and pair distance distribution function was well-matched with result of TEM analysis, except the high q region, which is caused by the polydispersity of tetrapod nanoparticles.

SAXS experiment were performed for hybrid and simple blend of tetrapod nanocomposite. Structure factors of hybrid and simple blend were deduced using form factor which was obtained experimentally. There was no significant changes of structure factors for hybrid except the very high concentration. At the high concentration, cluster or non-particular two phase trends was shown even though the surface of tetrapod nanocrystals were modified by brush polymers. The structure factor of blend, on the contrary, showed large cluster peaks and peaks for arm contact despite the concentration.

From these results, it is found that scattering method can characterize the dispersion structure of tetrapod nanocrystals, which is not only homogeneous dispersion structure but also the aggregation structure.

3.5. References

(1) Peter F. Green, Soft Matter, 2011, 7, 7914-7926

(2) Jenny Kim and Peter F. Green, Macromolecules 2010, 43, 1524-1529

(3) Guoqian Jiang, Russell J. Composto, ACS NANO, VOL. 6, NO. 2, 1578-1588, 2012

(4) Samanvaya Srivastava, Lynden A. Archer, Adv. Mater. 2014, 26, 201-234

(5) Jaehoon Lim, Lisa zur Borg, Kookheon Char, Rudolf Zentel, Macromol. Rapid Commun. 2014, 35, 1685-1691

(6) Matthias Zorn, Kookheon Char, ACS NANO, VOL. 3, NO. 5, 1063-1068, 2009

(7) Dongkyu Kim, Sangyong Jon, Nanotechnology 22 (2011) 155101

(8) Paschalis Alexandridis, Chem. Eng. Technol. 2011, 34, No. 1, 15-28

(9) Rudolf Zentel, Matthias Zorn, Nano Lett. 2010, 10, 2812-2816

(10) S. Alexander , J. Phys. 1977 , 38 , 983 .

(11) P. G. de Gennes , Macromolecules 1980 , 13 , 1069

(12) S. T. Milner , T. A. Witten , M. E. Cates , Macromolecules 1988 , 21 , 2610

(13) P. G. Ferreira , A. Ajdari , L. Leibler , Macromolecules 1998 , 31 , 3994

(14) Florian Mathias, Rudolf Zentel, Macromol. Rapid Commun. 2015, 36, 959-983

(15) Sanat K. Kumar et.al, Macromolecules (2010)

(16) Peter F. Green et.al, Langmuir (2010)

(17) Peter F. Green et.al, Macromolecules (2010)

(18) J.S. Pedersen, Adv. Colloid Interface Sci. 70 (1997) 171-210.

(19) R. J. Roe, Methods of x-ray and neutron scattering in polymer science, (2000)

(20) Jaehoon Lim, Kookheon Char, Chem. Mater. 2013, 25, 1443-1449.

(21) Marc Eberhardt, P. Theato, European Polymer Journal 41 (2005) 1569
(22) P. Theato, J. POLYM. SCI. PART A: POLYM. CHEM.: VOL. 46 (2008) 6677
(23) OTTO GLATTER, J. Appl. Cryst. (1977). 10, 415-421
(24) A. Bergmann, G. Fritz and O. Glatter, J. Appl. Cryst. (2000). 33, 1212-1216
(25) Gerhard Fritz and Otto Glatter, J. Phys.: Condens. Matter 18 (2006) S2403-S2419

Chapter 4. Placement Control of Tetrapod Nanoparticle within Colloidal Polymer Particles

4.1. Introduction

Like the other inorganic nanomaterials, tetrapod nanocrystals may as well be composite with functional organic materials for the practical processability and synergistic functionality originating from the interaction of these materials[1-4]. Depending on the applications, different dispersion structures are preferred for drawing the properties of tetrapod nanocrystals and maximizing the synergistic effects. Well-dispersion structure without aggregation of tetrapod nanocrystals is ideal for utilization of own unique properties of tetrapod nanocrystal or efficient interaction with neighboring organic materials. However, for the applications using the electrical properties of tetrapod nanocrystals, localization of tetrapod nanocrystal without aggregation would be effective to construct the bi-connected channel for charge transfer.

Dispersion structure of inorganic nanomaterials can be controlled by surface modification of inorganic nanomaterials with polymer brush which configures the inter-digitation with matrix polymer[5-8]. Lots of results about homogeneous dispersion of surface-modified inorganic QD or nanorods within polymer matrix are reported and Char and Zentel et al. reported that homogenously dispersed tetrapod nanocomposite with semiconducting block copolymers for solar cell application[9]. However, since the typical surface modification method with brush polymer enhances the compatibility between the matrix polymer and entire surface of tetrapod, usually the homogenous dispersion of inorganic nanoparticles is induced. Therefore, for the placing of tetrapod nanoparticles where we want, additional conditions or treatments should be involved besides the surface modification. Peter F green et al. shows that anisotropic dispersion which is the

dispersion structure of nanoparticles placed at the surface of polymer matrix without aggregation is realized by controlling the radius of nanoparticle[10]. In this results, the brush conditions are controlled to be not enough to accommodate the nanoparticles within polymer matrix and at the same time enough to overcome the van der Waals attractive force between nanoparticles. Rudolf Zentel et al. proposed the local demixing method for materialization of percolated structure[11]. These methods for Selective dispersion controlled by compatibility between the particles and matrix is locationally restricted to the interface, or hardly controllable because it is the results of non-equilibrium processes.

Meanwhile, "bottom up" approaches, which is also proposed by Rudolf Zentel et al., using the internally structured colloids of organic/inorganic hybrids, can place the inorganic nanoparticles to everywhere by various post treatments of colloidal particles[12]. For the hybrid colloidal particles which are the composite of colloidal polymer particles and inorganic nanoparticles, Joseph L. Keddie et al. report that the inorganic nanoparticles can be placed at the surface of colloidal polymer particles by hetero-flocculation of polymer colloid and inorganic nanoparticles[13] and Stefan A. F. Bon and Patrick J. Colver et al. present that hybrid colloidal particles which is covered with the inorganic particles are formed as the result of polymerization of hybrid colloidal particles in the pickering emulsion[14, 15].

However, the previous results involves the complexity of system due to polymerization with inorganic nanoparticles or introducing the moieties for hetero-flocculation. In this paper, we will present the results of incorporation of tetrapod nanoparticles at the inside and surface of polymer particles using block copolymer polymers which have anchoring groups for surface modification as well as amphiphilic moieties for colloidal stability.

Block copolymers for surface modification of inorganic nanoparticles are consisted with anchoring blocks for bonding to surface of nanoparticles and brush blocks for compatibility with

matrix polymers. The RAFT polymerization method, which is a sort of the living or controlled radical polymerization, is suitable for synthesizing the block copolymers which have any functional blocks and molecular weight with the appropriate chain transfer agent. P. Theato et al. report that diverse functional groups which contain the amine functional group can be adopted polymer chains by introducing the pentafluorophenylacrylate block to the polymer and substituting the active ester of pentafluorophenyl groups[16,17]. Therefore the block copolymers whose main chains are served as brush polymer and second block is the pentafluorophenylacrylate block are sequentially synthesized by RAFT polymerization, followed by substitution of pentafluorophenyl using amine with anchoring group, then the block copolymer having anchoring groups for surface modification of tetrapod nanocrystals is achieved. Furthermore, because the amine for introducing the anchoring groups are reminded in the second block as amide, if the main chain of block copolymer is non-polar, the block copolymer is supposed to facilitate the amphiphilic properties.

In the present study, the block copolymer whose main chain is polystyrene and second block has disulfide anchoring groups introduced by substitution of pentafluorophenyl with cysteamine methyl disulfide, Polystyrene-b-Poly (Cysteamine Methyl Disulfide) diblock copolymer (Figure 4.1), was used for brush and matrix polymer. Because of non-polar PS main chain and polar amide groups in the CMD block, the block copolymer shows the amphiphilic properties and does not be precipitated during typical precipitation process of polystyrene (which is precipitated with irregular shape, Figure 4.2-c) but forms the colloidal globular polymer particles (Figure 4.2-b) within polar solvent because the polar amide functional groups in CMD block are aligned toward outside of polymers and stabilize the polymer particles in the polar solvent (Figure 4.2). If surface modified tetrapod nanocrystals are present in this process, tetrapod-incorporated hybrid colloidal particles can be achieved.

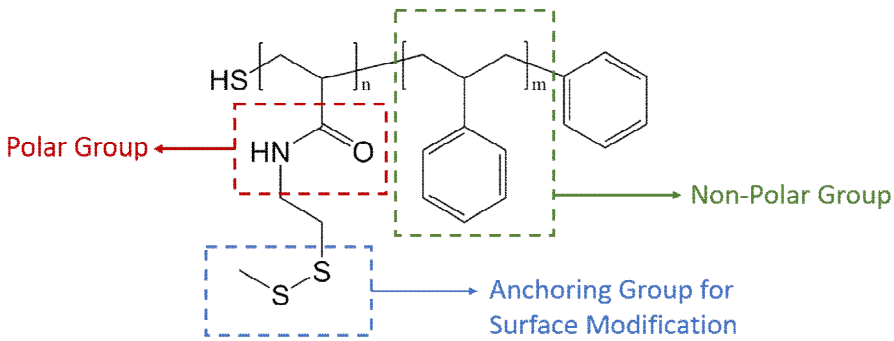

Polystyrene-b-Poly(Cysteamine Methyl Disulfide) Diblock Copolymer.

Figure 4.1 Chemical structure and functional moieties of PS-b-CMD block copolymers used in the present study. Polar amide groups in the CMD block and the non-polar polystyrene blocks facilitate the amphiphilic properties in selective solvents.

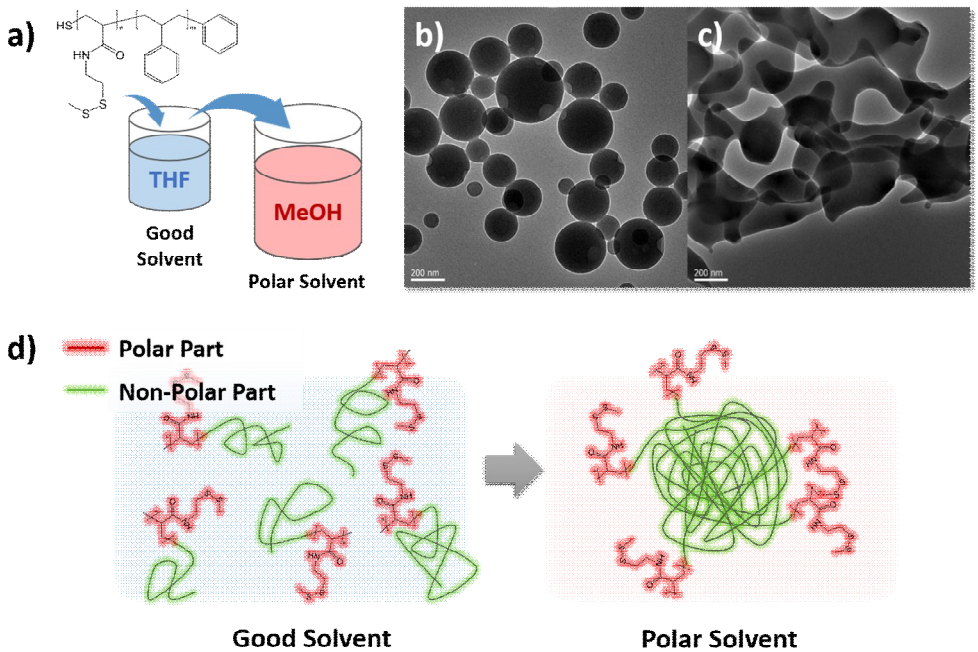

Figure 4.2 Surface-active behavior of PS-b-CMD block copolymers in a polar solvent. The PS-b-CMD block copolymers form colloidal polymer particles (b) during the typical precipitation process in a non-solvent for PS block (a) while forming chain precipitates with PS homopolymer alone, as shown in (c). The polar moieties in the PS-b-CMD block copolymers stabilize non-polar polystyrene block chains in a polar solvent, as schematically depicted in (d).

4.2. Experimental Section

4.2.1 Synthesis of Tetrapod Nanoparticles and Multi-Functional Block Copolymer

The CdSe tetrapods were synthesized by the continuous precursor injection method.[18] The arm length and radius of tetrapod was used in this study were 50 nm and 3 nm, respectively. The block copolymer whose main chain is polystyrene and second block has disulfide anchoring groups introduced by substitution of pentafluorophenyl with cysteamine methyl disulfide, Polystyrene-b-Poly (Cysteamine Methyl Disulfide) diblock copolymer (Figure 4.1), was used for brush and matrix polymer. It was prepared by first synthesizing a polystyrene-b-poly(pentafluorophenylacrylate) copolymer through the reversible addition fragmentation chain-transfer (RAFT) polymerization, and followed by the substitution of pentafluorophenyl units using cystemaine methyl disulfide(CMD) to obtain the PS-b-PCMA (Figure 4.1). The block copolyemrs having different molecular weight of the PS block being 300 and 50 were prepared with the same number of CMA repeat units of 5.

All the tetrapod nanocrystals and block copolymers are synthesized as described in the literatures[16-18] as likes with chapter 3.

4.2.2 Forming the Colloidal Polymer Particles

Colloidal Polymer Particles of the block copolymers were prepared by dropping the PS-b-PCMD solution of THF into methanol, which is general scheme for precipitation of polymer. The size of the colloidal polymer particles were controlled by polymer concentration in THF and solvent polarity (THF/methanol volume ratio) as well as polymer concentration within THF. DLS was used for characterization of radius of colloidal polymer particles.(Figure 4.6)

Tetrapod incorporated polymer particle were obtained by precipitation process, same with above mentioned, for the block

copolymer and surface modified tetrapod nanoparticles. For the incorporation of CdSe tetrapod nanocrystals within colloidal polymer particles, CdSe tetrapod nanocrystals and PS-b-PCMD block copolymers with excess amount were dissolved in THF and stirred for 12 hrs for surafec modification of tetrapod nanocrystal. After that, the solution was added to methanol dropwise, and then, the tetrapod-incorporated colloidal polymer particles were prepared.

The number of tetrapod nanoparticles in the colloidal polymer particles were controlled by weight ratio of polymer and tetrapod nanoparticles. The morphology and the distribution of colloidal particles and tetrapod nanocrystals were investigated by TEM analysis. TEM samples were prepared by dropping the colloidal solution onto a TEM grid followed by the evaporation of solvent.

4.3. Results and Discussion

When the PS-b-PCMD solution in THF (5 mL, 1 mg/mL) added into the methanol (45 mL), though it is a standard procedure of typical precipitation for polymers, block copolymer chains did not precipitated and form the colloidal particles. It was presumed that the PS-b-PCMD block copolymers were form the micellar polymer particle due to the polar PCMD block forming the corona (Figure 4.2). Similarly, the hybrid tetrapod nanocrystal whose surface was modified by the block copolymer chains incorporate this procedure and the colloidal polymer particles were formed with incorporating the tetrapod nanocrystal.

The result of analysis for hybrid nanostructures are shown in Figure 4.4. When a 5 mL THF solution containing CdSe tetrapod and PS50-b-PCMD5 was added into 45 mL of methanol, relatively small colloidal particles were observed and the tetrapod nanocrystals were incorporated inside the polymer particels individually (Figure 4.4a), with one tetrapod per package. However when PS300-b-PCMA5 was used instead of the PS50-b-PCMA5, polymer particles were extensive aggregated and all the tetrapod nanocrystals placed at the surface of nanocrystals, which is opposite position with PS50-b-PCMD5.

When the polarity of solvent medium was increased by changing the THF/methanol ratio to 10:40, the samples of PS50-b-PCMA5 make the larger polymer particles, and the number of tetrapod nanocrystals per polymer particles were increased. In the case of PS300-b-PCMA5, the size of polymer particles were little increased then the case of PS50-b-PCMA5, but the placement of tetrapod nanocrystal was holding and the number of tetrapod nanocrystals per polymer particles were increased, which is same with the case of low polarity solvent.

It is presumed that the difference of placement of tetrapod with molecular weight of block copolymer is caused by degree of inter-digitation brush polymer and matrix polymer. The chains of block copolymer moved freely in good solvent, are extracted and shrunk

with entanglement in polar solvent. If both polymer chains are inter-penetration deeply enough in good solvent, these chains are extracted and entangled together in polar solvent and tetrapods are incorporated at the inside of polymer particles. On the contrary, if both chains cannot or slightly penetrate to each other in good solvent, they are shrunk separately in polar solvent. However, As mentioned above, since the tetrapod whose surface is modified with PS(300)-b-CMD is well-dispersed homogeneously within same polymer matrix, there would be interpenetrations between both brushes, though it was not enough for co-particulation in polar solvent.

These hybrid colloidal particles which incorporate the tetrapod nanocrystals at inside or surface are the isotropic and anisotropic dispersion structures of micro-scale nanocomposite respectively and they can be used for the pieces of dispersion structure controllable macro-scale nanocomposite. We expect that hybrid colloidal particles of surface-placed tetrapod can construct the bi-connected channel for charge transfer by the post process, like as packing or sintering, and the connectivity can be controlled by particle size and content of tetrapod nanocrystals. Hybrid colloidal particles of inside-placed tetrapod is also expected to achieve the homogeneously dispersed structure. However, unlike dispersion structure of surface modified-tetrapod within bulk polymer matrix, the number density of tetrapod nanocrystals can be controlled by polymer particles and the number of tetrapod in the polymer particles.

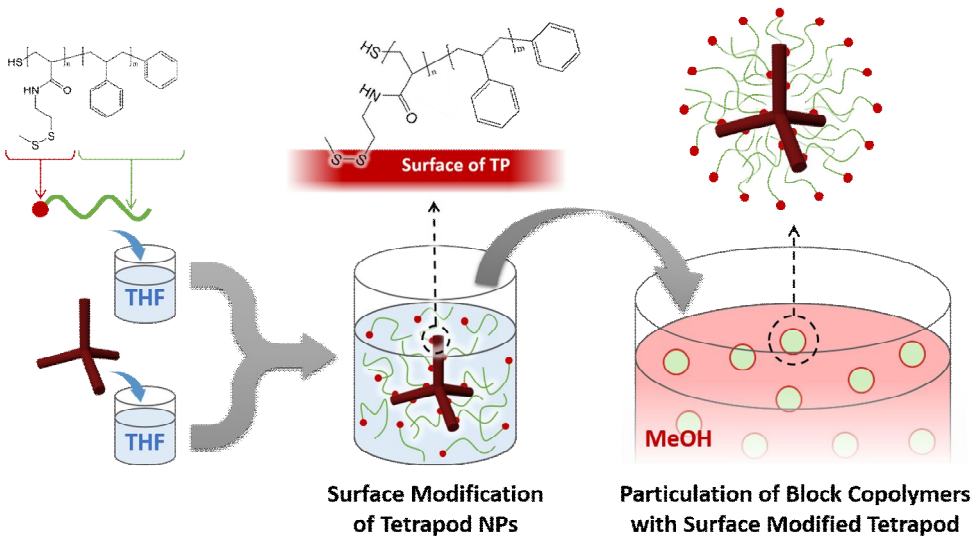

Figure 4.3 Incorporation of tetrapod (TP) nanocrystals within polymer particles. After the surface modification of TPs, the excess block polymers form colloidal particles with the surface-modified TPs in a polar solvent.

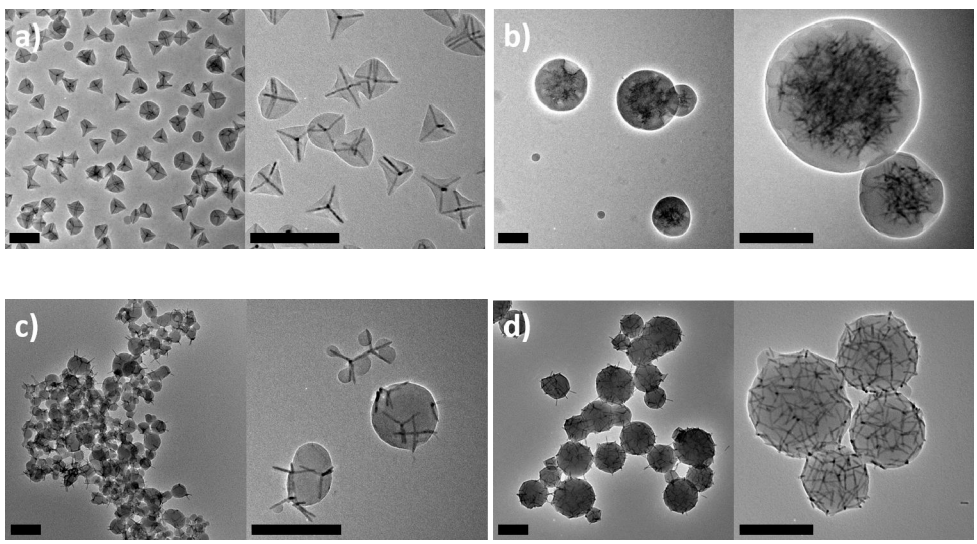

Figure 4.4 Tetrapod-Incorporated polymer particles. Tetrapods are located at the inside of the particles for PS(50)-b-CMD(a, b) and at the surface of the particles for PS(300)-b-CMD(c, d). Size of the polymer particles and the number of tetrapods in a particle are controlled by the volume ratio of THF and methanol(a, c : 5ml-THF/45ml-MeOH ; b, d : 10ml-THF/40ml-MeOH). Scale bar = 200nm

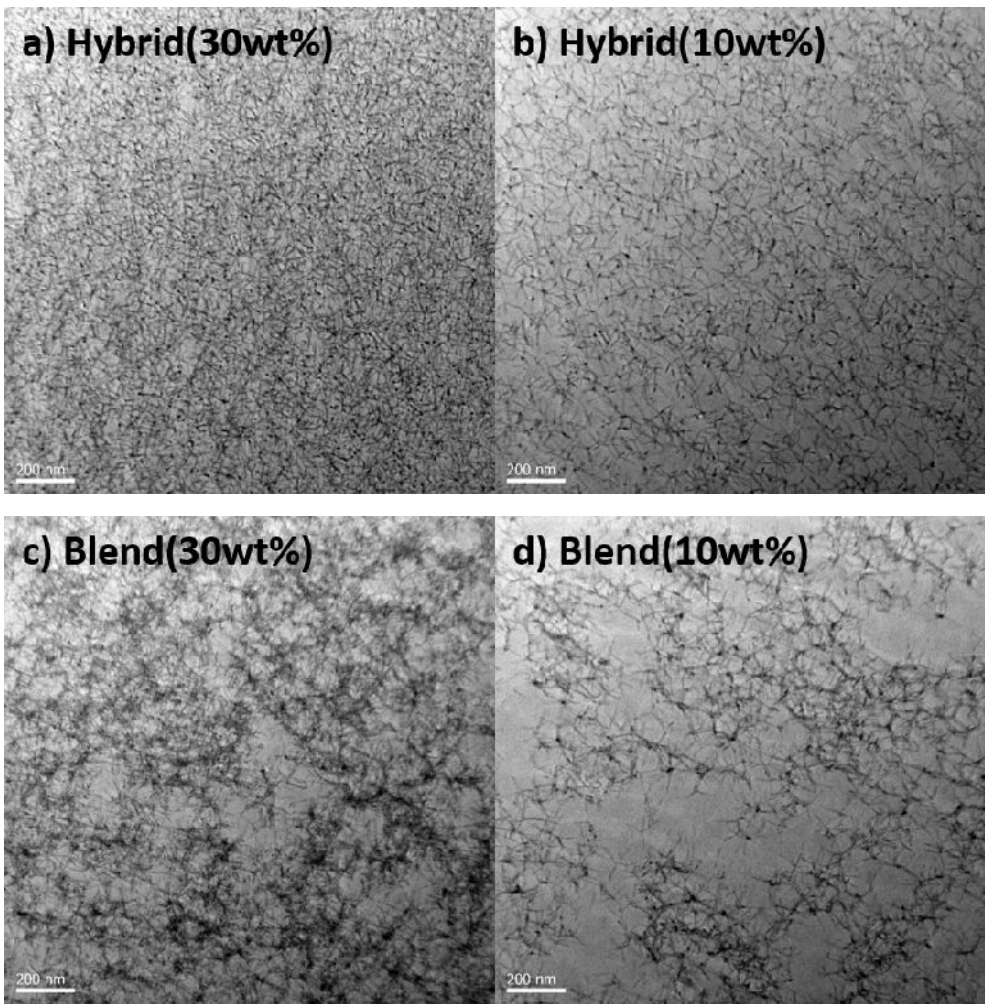

Figure 4.5 TEM images for hybrids and blends. The polymer for surface modification and bulk matrix of hybrids (a & b) is PS(300)-b-CMD diblock copolymer and the matrix polymer for blend (c & d) is PS(300) homopolymer. TPs are dispersed in matrix polymer homogeneously for hybrids(a & b) while TPs are aggregated for blends (c & d). Scale bar = 200 nm

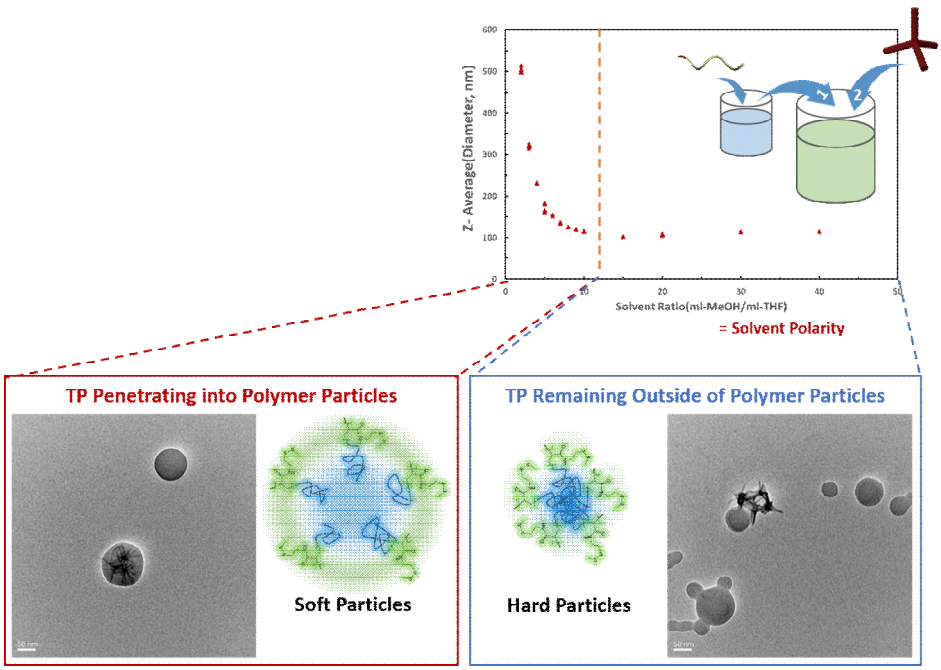

Figure 4.6 Path difference of incorporating tetrapod nanoparticles accorfing to polarity of solvent.

4.4. Conclusion

In this chapter, results for the placement control of CdSe tetrapod nanocrystals within PS-based block copolymer particles was presented. The placement of CdSe tetrapod nanocrystals was controlled by varying the molecular weight of the brush polymer and the polarity of solvent used for the particle preparation.

When small molecular weight brush polymer are used, tetrapod nanocrystals were placed at the interior of polymer particles, with more polar nanoprecipitation conditions leading to more finely divided polymer-tetrapod hybrid particles, as seen through TEM. Meanwhile, the tetrapod nanocrystals were placed on the surface of polymer particles when the brush polymer have high molecular weight, an observation which is attributed to the poor interdigitation between longer polymer chains prior to nanoprecipitation. Using the two distinct handles for controlling the spatial placement and distribution of tetrapods in the blend of tetrapod nanocrystal and polymer, various well-defined building blocks for a macro-scale assembly of electronic materials could be envisioned.

4.5. References

(1) Matthias Zorn, Kookheon Char, ACS NANO, VOL. 3, NO. 5, 1063-1068, 2009

(2) Dongkyu Kim, Sangyong Jon, Nanotechnology 22 (2011) 155101

(3) Paschalis Alexandridis, Chem. Eng. Technol. 2011, 34, No. 1, 15-28

(4) Rudolf Zentel, Matthias Zorn, Nano Lett. 2010, 10, 2812-2816

(5) S. Alexander , J. Phys. 1977 , 38 , 983 .

(6) P. G. de Gennes , Macromolecules 1980 , 13 , 1069 .

(7) S. T. Milner , T. A. Witten , M. E. Cates , Macromolecules 1988 , 21 , 2610.

(8) P. G. Ferreira , A. Ajdari , L. Leibler , Macromolecules 1998 , 31 , 3994 .

(9) Friederike Schmid and Kookheon Char and Rudolf Zentel, Macromol. Rapid Commun. 2014, 35, 1685

(10) X. C. Chen, P. F. Green, Soft Matter, 2011, 7, 1192

(11) Florian Mathias, Rudolf Zentel, Macromol. Rapid Commun. 2015, 36, 959

(12) M. B. Bannwarth , K. Landfester , Angew. Chem. Int. Ed. 2013 , 52 , 10107

(13) T. Wang , J. L. Keddie , Adv. Colloid Interface Sci. 2009 , 147–148 , 319 .

(14) Cauvin S, Colver PJ, Bon SAF. Macromolecules 2005, 38,

(15) Bon SAF, Colver PJ. Langmuir 2007, 23, 8316.

(16) Marc Eberhardt, P. Theato, European Polymer Journal 41 (2005) 1569

(17) P. Theato, J. POLYM. SCI. PART A: POLYM. CHEM.: VOL. 46 (2008) 6677 (8) Li, F.; Josephson, D. P.; Stein, A. Angew. Chem., Int. Ed. 2011, 50 (2), 360-388.

(18) Jaehoon Lim, Kookheon Char Chem. Mater. 2013, 25, 1443-1449.

초 록

무기 나노입자는 크기 및 형태로부터 기인한 그들의 독특한 전기전, 광학적 특성으로 인해 크기 및 형태가 일정한 입자의 합성 그 독특한 특성의 해석에 대한 연구가 활발히 진행되어 왔다. 특히 테트라포 나노크리스탈의 경우 그들의 특이한 형태에 기인하여, 주변 물질과 반응할 수 있는 넓은 표면적과 연결구조 형성의 용이성으로 인해 많은 관심을 받고 있다.

고분자 매질 내 무기 나노입자의 분산은 무기 나노입자의 고유의 특성을 발현하는데 매우 중요한 요소이다. 고분자 물질로 무기 나노입자의 표면을 치환하는 유/무기 하이브리드 방법은 무기 나노입자의 고른 분산을 유도하는데 적절한 방법이다. 하지만 다양한 방법을 통해 무기나노입자의 분산 특성을 조절한다 하여도 이러한 분산구조에 대한 정확한 해석이 되지 못하면, 분산 기술의 신뢰성을 확보할 수 없다. 일반적으로 분산 구조에 대한 분석은 microscopic 방법이 사용되지만, 최근들어서 분산 구조의 ensemble average를 측정할 수 있는 scattering method를 이용한 분산구조의 분석이 수행되고 있다.

따라서 본 연구에서는 테트라포드 무기 나노입자의 분산구조를 scattering method를 이용하여 분석하고자 하였고, 또한 하이브리드를 이용하여 테트라포드 나노입자의 분산구조를 조절하고자 연구를 진행하였다.

Chapter 1 에서는 테트라포드 무기 나노입자 및 유/무기 하이브리드, 그리고 scattering method를 이용한 분산 구조 분석에 대해 소개하였다.

Chapter 2 에서는 scatting method를 통한 테트라포드 무기 나노입자의 분산 구조 분석을 위해 테트라포드의 scattering model을 이론적 계산을 통해 제시하였다. 테트라포드의 네 개의 팔의 크기 및 형태가 같고, 그 끼인각이 모두 같은 규칙적 구조를 이용하여 모델을 단순할 할 수 있었다. 테트라포드는 비등방성 구조를 가지고 있기

때문에 random 배향을 고려하기 위해서는 적어도 3방향의 회전에 대한 고려가 필요했으며 이를 위해 테트라포의 이등분선을 축으로 하는 회전을 추가로 고려해주었다. 이렇게 구한 테트라포트의 scattering model을 이용하여 테트라포드의 scattering intensity 및 pair distance distribution function을 numerical method를 이용하여 제시하였다. 이렇게 제시된 model은 numerical 계산, 시뮬레이션, 그리고 small angle x-ray scattering 실험을 통해 검증되었다.

Chapter 3에서는 고분자 매질에 분산되어 있는 테트라포드 무기 나노입자의 분산특성을 small angle x-ray scattering 실험을 통해 분석하였다. 무기 나노입자의 분산구조는 그들 고유의 특성을 발현하는데 가장 중요한 요소이기 때문에 분산 특성 분석은 반드시 검증되어야 한다. 테트라포드의 형태 및 크기에 대한 정보를 가지고 잇는 form factor는 테트라포드를 용매에 분산시켜 얻을 수 있었고, 이를 이용하여 고분자 매질 내에 분산되어 있는 테트라포드의 분산 특성, 즉 structure factor를 구할 수 있었다. 테트라포드의 고른 분산을 유도하기 위한 하이브리드는 무기 나노입자와의 결합 특성을 같은 기능기를 갖는 블록공중합체를 합성하여 사용하였다.

Chapter4에서는 테트라포드에 대한 고분자 매질 및 고분자 입자 내 분산 특성 조절에 대한 연구를 진행하였다. 테트라포드의 표면 치환 및 고분자 입자 형성을 위한 다기능성 블록공중합체를 합성하여 사용하였다. 이러한 블록공중합체는 polystyrene main chain과 amide 기능기를 동시에 가지고 있어 양친성을 가지기 때문에 polar 용매 내에서 입자를 형성하게 된다. 이러한 블록 공중합체를 테트라포드와 함께 입자로 만들면 테트라포드가 들어있는 고분자 입자가 형성되며, 이러한 입자의 크기는 블록 공중합체의 농도 및 용매의 polarity로 조절 가능하고, 고분자 입자에 들어가는 테트라포드의 개수는 사용되는 블록 공중합체와 테트라포드 나노입자의 무게 비율로 결정된다.

주요어 : 테트라포드 무기 나노입자, 블록 공중합체, 하이브리드, 소각 엑스선 산란, 분산 구조
학 번 : 2012-30255